10608 *Inorg. Chem.* **2009**, *48*, 10608–10624
DOI: 10.1021/ic9011026

Inorganic Chemistry
Article

Topological Dependence of the Magnetic Exchange Coupling in Arylethynyl-Bridged Organometallic Diradicals Containing $[(\eta^2\text{-dppe})(\eta^5\text{-}C_5Me_5)Fe^{III}]^+$ Fragments

Frédéric Paul,*,† Arnaud Bondon,‡ Grégory da Costa,‡ Floriane Malvolti,† Sourisak Sinbandhit,† Olivier Cador,† Karine Costuas,† Loic Toupet,§ and Marie-Laure Boillot⊥

†*Sciences Chimiques de Rennes, UMR CNRS 6226, Université de Rennes 1, Campus de Beaulieu, Bât. 10C, 35042 Rennes Cedex, France,* ‡*PRISM, UMR CNRS 6026, Université de Rennes 1, CS 34317, Campus de Villejean, 35043 Rennes Cedex, France,* §*Institut de Physique de Rennes (IPR), UMR CNRS 6251, Université de Rennes I, Campus de Beaulieu, 35042 Rennes Cedex, France, and* ⊥*ICMMO, Equipe Chimie Inorganique, UMR CNRS 8182, Bât. 420, Université Paris-Sud 11, 91405 Orsay Cedex, France*

Received June 9, 2009

We have investigated the spin distribution and determined the magnetic exchange coupling J_{ab} (defined according to the following Hamiltonian: $\hat{H}_{spin} = -2J_{ab}\hat{S}_a \cdot \hat{S}_b$) for three arylethynyl-bridged organoiron(III) diradicals containing $[(\eta^2\text{-dppe})(\eta^5\text{-}C_5Me_5)Fe^{III}]^+$ fragments. Considering the distance separating the Fe^{III} centers ($\geq$11 Å), remarkably large intramolecular magnetic interactions between unpaired spins were found for two of them. Thus, an antiferromagnetic coupling (J_{ab}) of ca. -190 cm^{-1} was experimentally determined for the binuclear Fe^{III} species featuring a 1,4-diethynylbenzene bridge **1**$[PF_6]_2$, while a ferromagnetic interaction of over $+150$ cm^{-1} was evidenced for its 1,3-substitued analogue **2**$[PF_6]_2$. We also show that a much weaker interaction ($0 > J_{ab} \geq -1$ cm^{-1}) takes place in the 4,4′-biphenyl analogue of **1**$[PF_6]_2$ (**3**$[PF_6]_2$), evidencing that insertion of an additional 1,4-phenylene unit in the bridge severely disrupts the magnetic communication in these diradicals. With the help of NMR and density functional theory, the magnetic properties of these compounds were rationalized and compared to those of the corresponding mononuclear Fe^{III} relatives **4**$[PF_6]$ and **5**$[PF_6]$. Finally, it is shown that, for all of these dinuclear Fe(III) complexes, the structural changes between singlet and triplet spin isomers remain very small regarding the carbon-rich bridge. Thus, even for a strongly coupled diradical such as **1**$[PF_6]_2$, a dominant diradicaloid character dominates the valence-bond description of the singlet state unpaired electrons.

Introduction

During this past decade, organometallics featuring redox-active centers σ-ligated to a carbon-rich bridging ligand have aroused a lot of interest for molecular electronics, mostly because of their outstanding properties from the electron-transfer perspective but also, more recently, because of their remarkable magnetic properties.[1,2] Since the seminal contribution of Crutchley and co-workers, who reported the existence of very strong magnetic interactions taking place over quite long distances in several open-shell representatives of this peculiar class of compounds,[3,4] the exploration of the magnetic properties of such organometallic polyradicals has

*To whom correspondence should be addressed. E-mail: frederic.paul@univ-rennes1.fr. Tel.: (+33) 02 23 23 59 62. Fax: (+33) 02 23 23 56 37.

(1) (a) Gao, L.-B.; Liu, S.-H.; Zhang, L.-Y.; Shi, L.-X.; Chen, Z.-N. *Organometallics* **2006**, *25*, 506–512. (b) Gao, L.-B.; Zhang, L.-Y.; Shi, L.-X.; Chen, Z.-N. *Organometallics* **2005**, *24*, 1678–1684. (c) Mahapatro, A. K.; Ying, J.; Ren, T.; Janes, D. B. *Nano Lett*. **2008**, *8*, 2131–2136. (d) Qi, H.; Ghupta, A.; Noll, B. C.; Snider, G. L.; Lu, Y.; Lent, C. S.; Fehlner, T. P. *J. Am. Chem. Soc*. **2005**, *127*, 15218–15227. (e) Blum, A. S.; Ren, T.; Parish, D. A.; Trammell, S. A.; Moore, M. H.; Kushmerick, J. G.; Xu, G.-L.; Deschamps, J. R.; Polack, S. K.; Shashidar, R. *J. Am. Chem. Soc*. **2005**, *127*, 10010–10011. (f) Xu, G.-L.; Crutchley, R. J.; DeRosa, M. C.; Pan, Q.-J.; Zhang, H.-X.; Wang, X.; Ren, T. *J. Am. Chem. Soc*. **2005**, *127*, 13354–13365. (g) Cifuentes, M. P.; Humphrey, M. G.; Morrall, J. P.; Samoc, M.; Paul, F.; Roisnel, T.; Lapinte, C. *Organometallics* **2005**, *24*, 4280–4288. (h) Hu, Q. Y.; Lu, W. X.; Tang, H. D.; Sung, H. H. Y.; Wen, T. B.; Williams, I. D.; Wong, G. K. L.; Lin, Z.; Jia, G. *Organometallics* **2005**, *24*, 3966–3973. (i) Wong, W.-Y.; Che, C.-M.; Chan, M. C. W.; Han, J.; Leung, K.-H.; Phillips, D. L.; Wong, K.-Y.; Zhu, N. *J. Am. Chem. Soc*. **2005**, *127*, 13997–14007. (j) Venkatesan, K.; Blacque, O.; Fox, T.; Alfonso, M.; Schmalle, H. W.; Berke, H. *Organometallics* **2004**, *23*, 1183–1186. (k) Bruce, M. I.; Ellis, B. G.; Gaudio, M.; Lapinte, C.; Melino, G.; Paul, F.; Skelton, B. W.; Smith, M. E.; Toupet, L.; White, A. H. *J. Chem. Soc., Dalton Trans*. **2004**, 1601–1609. (l) Fraysse, S.; Coudret, C.; Launay, J.-P. *J. Am. Chem. Soc*. **2003**, *125*, 5880–5888. (m) Powell, C. E.; Humphrey, M. G.; Cifuentes, M. P.; Morrall, J. P.; Samoc, M.; Luther-Davies, B. *J. Phys. Chem. A* **2003**, *107*, 11264–11266.

(2) For reviews, see, for instance: (a) Szafert, S.; Gladysz, J. A. *Chem. Rev*. **2006**, *106*, PR1–PR33. (b) Ren, T. *Organometallics* **2005**, *24*, 4854–4870. (c) Powell, C. E.; Humphrey, M. G. *Coord. Chem. Rev*. **2004**, *248*, 725–756. (d) Rigaut, S.; Touchard, D.; Dixneuf, P. H. *Coord. Chem. Rev*. **2004**, *248*, 1585–1601. (e) Bruce, M. I.; Low, P. J. *Adv. Organomet. Chem*. **2004**, *50*, 179–444. (f) Ceccon, A.; Santi, S.; Orian, L.; Bisello, A. *Coord. Chem. Rev*. **2004**, *248*, 683–724. (g) Long, N. J.; Williams, C. K. *Angew. Chem., Int. Ed. Engl*. **2003**, *42*, 2586–2617. (h) Yam, V. W.-W. *Acc. Chem. Res*. **2002**, *35*, 555–563. (i) Launay, J.-P.Coudret, C. In *Electron Transfer in Chemistry*; Balzani, V., de Silva, A. P., Eds.; Wiley-VCH: New York, 2000; Vol. *5*, pp 3−47. (j) Paul, F.; Lapinte, C. *Coord. Chem. Rev*. **1998**, *178*/*180*, 427–505. (k) Crutchley, R. J. *Adv. Inorg. Chem*. **1994**, *41*, 273–325.

(3) Aquino, M. A. S.; Lee, F. L.; Gabe, E. J.; Bensimon, C.; Greedan, J. E.; Crutchley, R. J. *J. Am. Chem. Soc*. **1992**, *114*, 5130–5140.

(4) Naklicki, M. L.; White, C. A.; Plante, L. L.; Evans, C. E. B.; Crutchley, R. J. *Inorg. Chem*. **1998**, *37*, 1880–1885.

 Published on Web 10/26/2009

been undertaken more systematically by an increasing number of research teams around the world.[5−8]

The contribution of our group in this field has been mostly focused on the synthesis and characterization of several new Fe^{III} polyradicals bearing "(η^2-dppe)(η^5-C_5Me_5)Fe−" end groups as $S = {}^1/_2$ spin carriers [dppe = 1,2-bis(diphenylphosphino)ethane] separated by carbon-rich spacers.[9−14] In a recent review, we have rationalized the magnetic properties of these organometallic polyradicals, which apparently bear strong analogies with their purely organic relatives.[11]

$$\hat{H}_{spin} = -2J_{ab}\hat{S}_a \cdot \hat{S}_b \qquad (1)$$

Some additional work was, however, needed to improve further our understanding of these fascinating paramagnetic species, especially those containing aryl groups inserted in the bridging ligand.[15−18] For instance, no magnetic susceptibility measurements have been performed yet on the most recently synthesized diradicals of that kind such as **3**$[PF_6]_2$,[17] while previous susceptibility measurements reported for **1**$[PF_6]_2$[12,19] were indicative of a seemingly too weak exchange coupling constant (J_{ab}; eq 1) in comparison to values determined more recently for related compounds.[9,10,16,20] Also, depending on the model complexes, on the starting geometry, and on the starting electronic density used (guess), density functional theory (DFT) computations [ADF program/generalized gradient approximation (GGA) exchange-correlation functional] always led to much larger gaps between spin states for **1**$[PF_6]_2$ and **2**$[PF_6]_2$ than those found experimentally, outlining the need to try an alternative DFT method to accurately model their magnetic properties.

Another important question more specific to compounds possessing *p*-phenylene units inserted in the carbon-rich bridge, such as **1**$[PF_6]_2$ and **3**$[PF_6]_2$, concerns the importance of the structural rearrangement taking place for the carbon-rich bridge between their triplet and singlet states.[11] This rearrangement has been shown to be quite important for several related polyyne-bridged (d^5−d^5) organometallic homodinuclear species (Scheme 1a).[13,14,23,24] It is believed to result from the resonance between the open-shell singlet valence-bond (VB) mesomer and the closed-shell diamagnetic VB mesomer possessing one additional bond in the organic bridge. In this respect, the strong cumulenic/quinoidal character recently evidenced for the carbon-rich bridge in the diamagnetic (singlet) ground state (GS) of the 9,10-anthryl analogue (**6**$^{2+}$; Chart 1) of **1**$^{2+}$ suggests that large structural modifications of the bridge are also likely to take place when *p*-arylene units are inserted in it (Scheme 1b).[9,11] However, considering that the importance of this structural rearrangement is certainly strongly dependent on the nature and number of the *p*-arylene units present in the bridge, this point deserved to be specifically investigated with **1**$[PF_6]_2$ and **3**$[PF_6]_2$.

For all of these reasons, we have presently decided to revisit the magnetic properties of **1**$[PF_6]_2$ and **2**$[PF_6]_2$ and to study those of **3**$[PF_6]_2$, from both the experimental and theoretical standpoint, in order to arrive at a consistent description of these aryl-containing diradicals. To this aim, in addition to magnetic susceptibility measurements (SQUID), variable-temperature (VT) NMR measurements were envisioned as a means to obtain information about the singlet−triplet gaps. Indeed, this spectroscopy had often been successfully used to probe the intramolecular exchange coupling constants in solution for specific organic[25] or organometallic[13,26−28] diradicals. Then, as recently shown for the mononuclear Fe^{III} doublet ($S = {}^1/_2$) model complexes **4**$[PF_6]$ and **5**$[PF_6]$,[29] NMR also constitutes a convenient means to obtain experimental estimates of the atomic spin density delocalized from the metal center on the arylacetylide ligand. Indeed, since the pioneering works of Anderson and Köhler on organometallic (poly)radicals,[26,27,30]

(5) (a) Carlson, C. N.; Veauthier, J. M.; John, K. D.; Morris, D. E. *Chem.—Eur. J.* **2008**, *14*, 422–431. (b) Choukroun, R.; Lorber, C.; De Caro, D.; Vendier, L. *Organometallics* **2006**, *25*, 4243–4246. (c) Kheradmandan, S.; Heinze, K.; Schmalle, H.; Berke, H. *Angew. Chem., Int. Ed. Engl.* **1999**, *38*, 2270–2273. (d) Cargill Thompson, A. M. W.; Gatteschi, D.; Mac Cleverty, J. A.; Navas, J. A.; Rentschler, E.; Ward, M. D. *Inorg. Chem.* **1996**, *35*, 2701–2703.

(6) Fabre, M.; Bonvoisin, J. *J. Am. Chem. Soc.* **2007**, *129*, 1434–1444.

(7) (a) Bruce, M.; Costuas, K.; Ellis, B. J.; Halet, J.-F.; Low, P. J.; Moubaraki, B.; Murray, K. S.; Ouddaï, N.; Perkins, G. J.; Skelton, B. W.; White, A. H. *Organometallics* **2007**, *26*, 3735–3745. (b) Shi, Y.; Yee, G. T.; Wang, G.; Ren, T. *J. Am. Chem. Soc.* **2004**, *126*, 10552–10553.

(8) Kheradmandan, S.; Venkatesan, K.; Blacque, O.; Schmalle, H.; Berke, H. *Chem.—Eur. J.* **2004**, *10*, 4872–4885.

(9) de Montigny, F.; Argouarch, G.; Costuas, K.; Halet, J.-F.; Roisnel, T.; Toupet, L.; Lapinte, C. *Organometallics* **2005**, *24*, 4558–4572.

(10) Roué, S.; Le Stang, S.; Toupet, L.; Lapinte, C. *C. R. Chim.* **2003**, *6*, 353–366.

(11) Paul, F.; Lapinte, C. In *Unusual Structures and Physical Properties in Organometallic Chemistry*; Gielen, M., Willem, R., Wrackmeyer, B., Eds.; Wiley: San Francisco, 2002; pp 219−295.

(12) Le Narvor, N.; Lapinte, C. *C. R. Acad. Sci., Ser. IIc: Chim.* **1998**, 745–749.

(13) Bruce, M.; Costuas, K.; Davin, T.; Ellis, B. J.; Halet, J.-F.; Lapinte, C.; Low, P. J.; Smith, M. E.; Skelton, B. W.; Toupet, L.; White, A. H. *Organometallics* **2005**, *24*, 3864–3881.

(14) Jiao, H.; Gladysz, J. A.; Costuas, K.; Halet, J.-F.; Toupet, L.; Paul, F.; Lapinte, C. *J. Am. Chem. Soc.* **2003**, *125*, 9511–9522.

(15) Le Narvor, N.; Lapinte, C. *Organometallics* **1995**, *14*, 634–639.

(16) Weyland, T.; Costuas, K.; Mari, A.; Halet, J.-F.; Lapinte, C. *Organometallics* **1998**, *17*, 5569–5579.

(17) Ibn Ghazala, S.; Paul, F.; Toupet, L.; Roisnel, T.; Hapiot, P.; Lapinte, C. *J. Am. Chem. Soc.* **2006**, *128*, 2463–2476.

(18) Matsuura, Y.; Tanaka, Y.; Akita, M. *J. Organomet. Chem.* **2009**, *694*, 1840–1847.

(19) The samples of **1**$[PF_6]_2$ used for SQUID measurements were contaminated by paramagnetic impurities (presumably high-spin iron oxides), and fitting of the magnetic susceptibility data led to several possible J_{ab} values.[21] The lowest value was eventually retained based on common knowledge at that time.[22]

(20) Tanaka, Y.; Shaw-Taverlet, J. A.; Justaud, F.; Cador, O.; Roisnel, T.; Akita, M.; Hamon, J.-R.; Lapinte, C. *Organometallics* **2009**, *28*, 4656−4669.

(21) Lapinte, C. *Personal communication.*

(22) Coffman, R. E.; Buettner, G. R. *J. Phys. Chem.* **1979**, *83*, 2387–2392.

(23) (a) Zhou, Y.; Seyler, J. W.; Weng, W.; Arif, A. M.; Gladysz, J. A. *J. Am. Chem. Soc.* **1993**, *115*, 8509–8510. (b) Brady, M.; Weng, W.; Zhou, Y.; Seyler, J. W.; Amoroso, A. J.; Arif, A. M.; Böhme, M.; Frenking, G.; Gladysz, J. A. *J. Am. Chem. Soc.* **1997**, *119*, 775–788.

(24) Paul, F.; Meyer, W.; Jiao, H.; Toupet, L.; Gladysz, J. A.; Lapinte, C. *J. Am. Chem. Soc.* **2000**, *122*, 9405–9414.

(25) Kopf, P.; Morokuma, K.; Kreilick, R. *J. Chem. Phys.* **1970**, *54*, 105–110.

(26) Köhler, F. H.; Prössdorf, W.; Schubert, U. *Inorg. Chem.* **1981**, *20*, 4096–4101.

(27) Hilbig, H.; Hudeczek, P.; Kohler, F. H.; Xie, X.; Bergerat, P.; Kahn, O. *Inorg. Chem.* **1998**, *37*, 4246–4257.

(28) Cremer, C.; Burger, P. *J. Am. Chem. Soc.* **2003**, *125*, 7664–7677.

(29) Paul, F.; da Costa, G.; Bondon, A.; Gauthier, N.; Sinbandhit, S.; Toupet, L.; Costuas, K.; Halet, J.-F.; Lapinte, C. *Organometallics* **2007**, *26*, 874–896.

(30) (a) Anderson, S. E., Jr.; Drago, R. S. *J. Am. Chem. Soc.* **1970**, *92*, 4244–4254. (b) Köhler, F. H.; Hofmann, P.; Prössdorf, W. *J. Am. Chem. Soc.* **1981**, *103*, 6359–6372. (c) Köhler, F. H. In *Magnetism: Molecules to Materials*; Miller, J. S., Drillon, M., Eds.; Wiley-VCH: Weinheim, Germany, 2001.

(31) (a) Laidlaw, W. M.; Denning, R. G. *Chem. Commun.* **2008**, 1590–1592. (b) Fernandez, F. J.; Blacque, O.; Alfonso, M.; Berke, H. *Chem. Commun.* **2001**, 1266–1267. (c) Roger, C.; Hamon, P.; Toupet, L.; Rabaâ, H.; Saillard, J.-Y.; Hamon, J.-R.; Lapinte, C. *Organometallics* **1991**, *10*, 1045–1054.

Scheme 1. Effective (a) and Envisioned (b) Structural Rearrangements Taking Place between the Singlet and Triplet States of Carbon-Rich Diradicals with Various Bridges

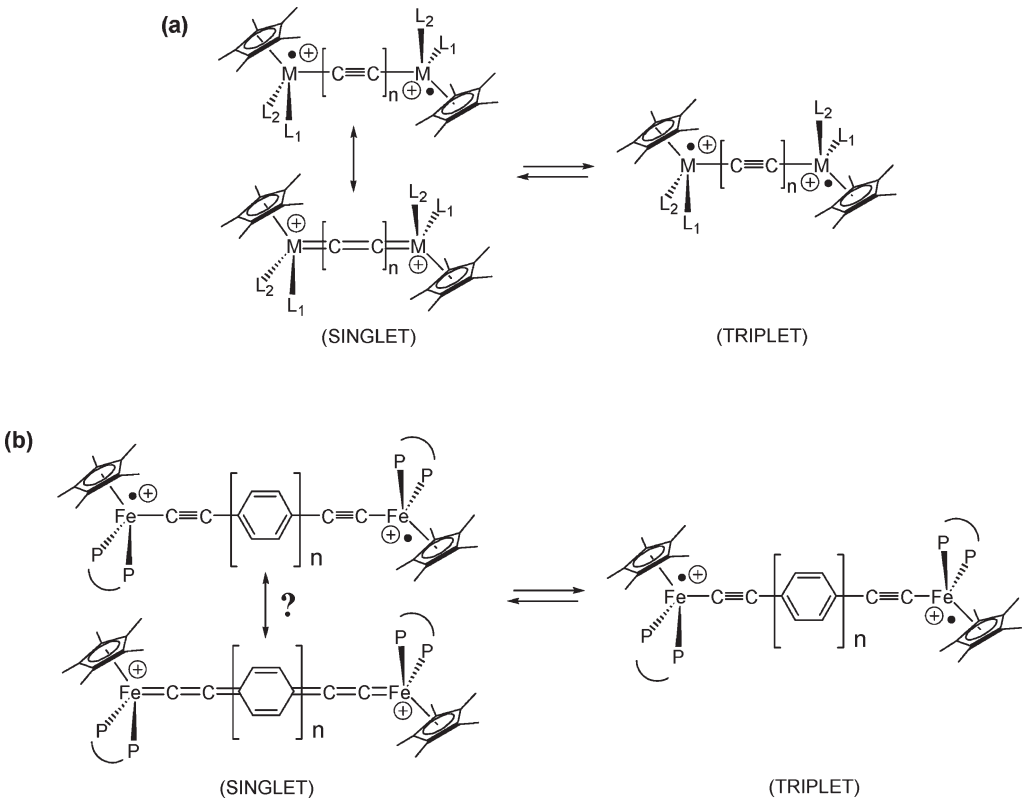

Chart 1. Selected Organoiron(III) Diradicals and Corresponding Model Monoradicals

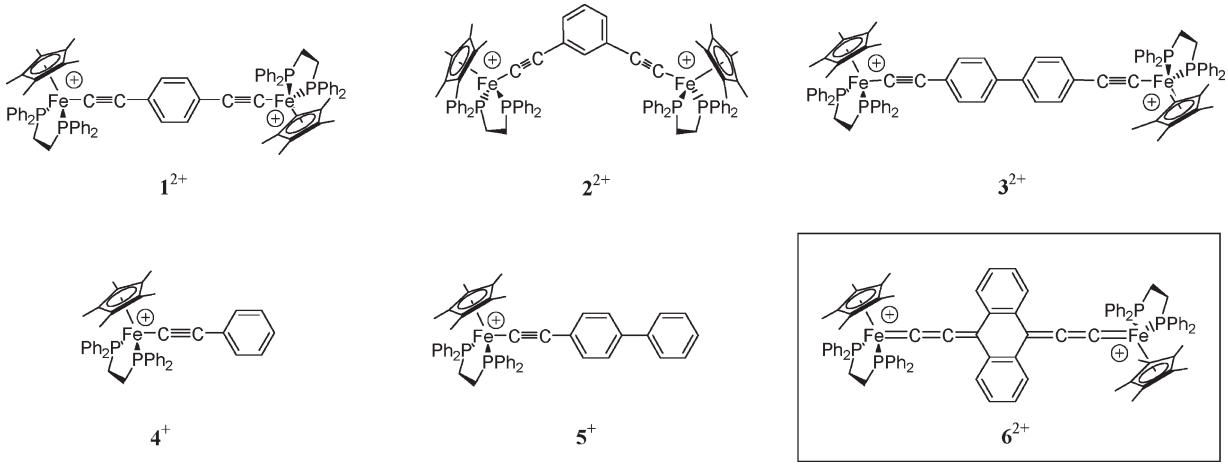

this spectroscopy has now become an attractive tool to investigate the electronic open-shell structures of polynuclear carbon-rich paramagnetic compounds.[8,16,24,26,28,31,32] With **1**−**3**-$[PF_6]_2$, this experimental technique should therefore help us in checking the consistency of any new DFT calculations undertaken on these diradicals. Moreover, its low sensitivity to the presence of paramagnetic impurities in the samples constitutes another particularly attractive feature for working with these reactive compounds.[26]

Thus, in order to achieve a better understanding of the magnetic properties of the organometallic diradicals **1**−**3**-$[PF_6]_2$ in relation to their electronic structures, we have now (i) measured their intramolecular exchange coupling constants (J_{ab}), (ii) investigated the specific structural changes between their singlet and triplet spin states by monitoring UV−vis−near-IR and related experimental signatures over relevant temperature ranges, (iii) experimentally determined the spin distribution on selected carbon atoms of the unsaturated spacer by NMR, and (iv) modeled the spin distribution and magnetic interactions in these diradicals by DFT using the Gaussian package and the B3LYP functional. This functional is one of the better-suited functionals to estimate J_{ab} values when the spin projection cannot be

(32) For studies concerned with conformational changes, see also: (a) Walter, M. D.; Berg, D. J.; Andersen, R. A. *Organometallics* **2007**, *26*, 2296–2307. (b) Walter, M. D.; Berg, D. J.; Andersen, R. A. *Organometallics* **2006**, *25*, 3228–3237. (c) Schultz, M.; Boncella, J. M.; Berg, D. J.; Don Tilley, T.; Andersen, R. A. *Organometallics* **2002**, *21*, 460–472.

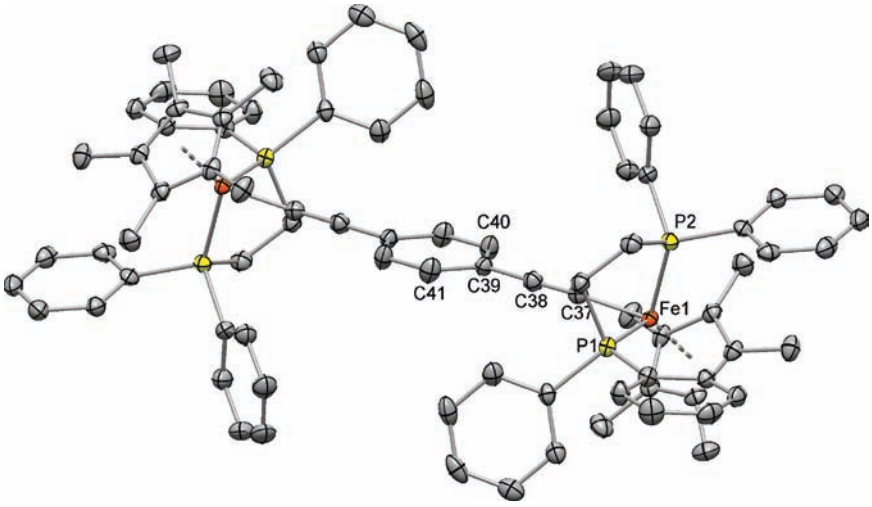

Figure 1. ORTEP representation of one dicationic molecule in $\mathbf{1}[PF_6]_2\cdot CH_2Cl_2$ at a 50% probability level. Hydrogen atoms have been omitted for clarity.

handled.[33] In light of these investigations, we subsequently discuss the relationship between J_{ab} and the spin distribution found for $\mathbf{1}-\mathbf{3}[PF_6]_2$, as well as the structural changes taking place between their spin states.

Results

Synthesis of $\mathbf{1}-\mathbf{3}[PF_6]_2$. The known Fe^{III} diradicals $\mathbf{1}-\mathbf{3}[PF_6]_2$ were obtained according to published procedures.[15−17] We were able to grow single crystals of $\mathbf{1}[PF_6]_2\cdot CH_2Cl_2$ by the slow diffusion of *n*-pentane into a dichloromethane solution of the corresponding complex, and the solid-state structure of this compound could be solved by X-ray diffraction (Figure 1). A brief discussion of the structural data of this diradical is given below.

Magnetic Susceptibility Measurements of $\mathbf{1}-\mathbf{3}[PF_6]_2$. The magnetic susceptibilities of $\mathbf{1}-\mathbf{3}[PF_6]_2$ have been measured between 10 and 300 K using crystalline samples of $\mathbf{1}[PF_6]_2$ and $\mathbf{3}[PF_6]_2$ and freshly prepared (amorphous) samples of $\mathbf{2}[PF_6]_2$. The thermal variation of the $\chi_M T$ product of these compounds, with χ_M being the molar magnetic susceptibility and T the temperature in Kelvin, is represented in Figure 2. These data were modeled with a modified Bleaney−Bowers law to take into account paramagnetic impurities (eq 2).[34,35] In eq 2, N, g, k, and β are the Avogadro number, the Zeeman factor, the Boltzmann constant, and the Bohr magneton, respectively. The amount x is calculated assuming that the paramagnetic impurities possess a spin of $S = {}^1/_2$.

$$\chi_M = (1-x)\frac{2Ng^2\beta^2}{kT}\frac{1}{3+\exp\left(-\frac{2J_{ab}}{kT}\right)} + x\frac{2Ng^2\beta^2}{3kT}S(S+1) \qquad (2)$$

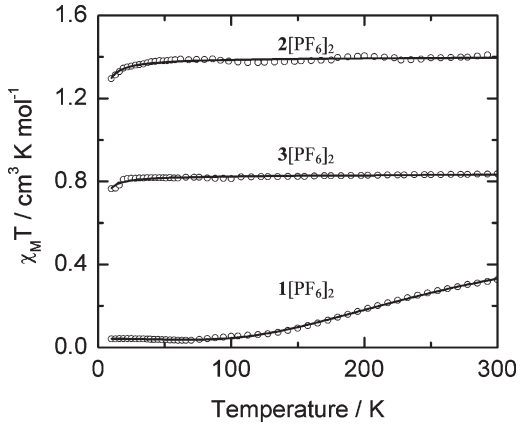

Figure 2. Thermal variation of $\chi_M T$ for powdered samples of $\mathbf{1}-\mathbf{3}[PF_6]_2$, with the best-fitted curves obtained using the modified Bleaney−Bowers equation (eq 2).

For $\mathbf{1}[PF_6]_2$, the curve is characteristic of a diamagnetic GS with a thermally accessible paramagnetic triplet state. In contrast to the previous attempts using powderish samples,[12,19] the fit provided a unique value for the exchange coupling constant (J_{ab}) defined according to eq 1.[11] A g value of 2.04 ± 0.01 and a J_{ab} value of -191 ± 3 cm^{-1} are given by the fitting procedure with $x = 11\%$.[35] For $\mathbf{2}[PF_6]_2$, $\chi_M T$ remains constant in the investigated temperature range and corresponds to a value of 1.4 cm^3 K mol^{-1} (Figure 2), which fits with a triplet GS ($S = 1$). In this case, the singlet−triplet gap cannot be determined using eq 2 but must be larger than 300 cm^{-1}. Indeed, fitting with a Curie−Weiss law gives a Curie constant of 1.394 ± 0.01 cm^3 K mol^{-1} and a θ value of -0.73 ± 0.04 K, which is only compatible with a triplet state possessing a g value of 2.37. A ferromagnetic exchange coupling (J_{ab}) of 150 cm^{-1} was thus considered in the following for this radical based on eq 1. It should, however, be kept in mind that this value constitutes a lower bound of J_{ab} in $\mathbf{2}[PF_6]_2$, with the preeminent feature of this diradical being that its triplet spin state is quite exclusively thermally populated at room temperature. Finally, the thermal variation of the $\chi_M T$ product of $\mathbf{3}[PF_6]_2$ is also almost constant (~0.82 cm^3 K mol^{-1}) in the investigated temperature range and coincides with the

(33) Ruiz, E.; Alvarez, S.; Cano, J.; Polo, V. *J. Chem. Phys.* **2005**, *123*, 164110–164117.

(34) Bleaney, B.; Bowers, K. D. *Proc. R. Soc. London, Ser. A* **1952**, *214*, 451–465.

(35) For all of these compounds, a partial decomposition over time into the known diamagnetic carbonyl complex $[(\eta^2\text{-dppe})(\eta^5\text{-}C_5Me_5)Fe(CO)][PF_6]$ was often stated.[36] This reaction, which involves paramagnetic intermediates, most likely originates from short (but presently unavoidable) exposures of the solid samples to air (oxygen) during handling and transfer.[37] In this respect, powderish samples of $\mathbf{2}[PF_6]_2$ proved to be much more reactive than crystalline samples of $\mathbf{1}[PF_6]_2$ and $\mathbf{3}[PF_6]_2$.

spin-only value expected for two uncoupled spins $S = {}^1/_2$. At temperatures lower than 20 K, $\chi_M T$ decreases slightly on cooling, which is characteristic of a small antiferromagnetic interaction between unpaired spins, but its amplitude is dramatically reduced in comparison to that operative in **1**$[PF_6]_2$. Fitting these data with eq 2 (in fixing $x = 0\%$) gives J_{ab} values of around -0.9 ± 0.1 cm^{-1} and g values of around 2.099 ± 0.002, with a value of 1 cm^{-1} constituting an upper bound of $|J_{ab}|$ for this antiferromagnetic interaction in **3**$[PF_6]_2$. Notably, with regard to the limited stability of the samples of **1**−**3**$[PF_6]_2$,[35] the g values issued from the various fitting procedures remain in an acceptable range when compared to those independently measured by electron spin resonance (ESR) or measured for related Fe^{III} complexes.[17]

Solid-State Structure of 1$[PF_6]_2 \cdot CH_2Cl_2$. The **1**$[PF_6]_2 \cdot CH_2Cl_2$ compound crystallizes in the $P2_1/c$ space group with two half-molecules in the asymmetric unit and two half-molecules of the dichloromethane solvate (see the Experimental Section and Figure 1). To investigate any structural change correlated to a change in the population of the singlet versus triplet spin states, the present data were recorded at low temperature (100 K) and at ambient temperature (293 K). The structure could be solved with fair accuracy in both cases (final $R = 5.0 \pm 0.2\%$). At 293 K, a significant expansion of the unit cell (from 7483 to 7736 Å^3) is observed along with a decrease in the calculated density (1.490 vs 1.441). Bond lengths and angles around the metal centers are unexceptional in comparison with published data for similar compounds. They compare quite well with bond distances previously reported for **3**$[PF_6]_2$ or for the mononuclear Fe^{III} compounds **4**$[PF_6]$ and **5**$[PF_6]$.[17,38] Concerning the carbon-rich bridge, the data would be consistent with a slight quinoidal deformation of the phenyl ring at low temperature accompanied by a slight lengthening of the acetylide spacer (C38−C39) and concomitant shortening of the Fe−C37 and C38−C39 bonds (Supporting Information), in line with expectations based in Scheme 1b. However, these changes are weak and remain within experimental uncertainty [3 estimated standard deviations (esd's)] for most atoms of the bridge.

VT Spectroscopic Study of 1$[PF_6]_2$ and 2$[PF_6]_2$. In order to gain some insight in the electronic/bonding modifications accompanying the change in spin-state populations (Scheme 1b), the UV−vis−near-IR spectra of **1**$[PF_6]_2$ and **2**$[PF_6]_2$ were monitored between 10 and 300 K in the solid state (KBr pellets). According to its J_{ab} value, **1**$[PF_6]_2$ should present large changes in its spin-state population in the temperature range investigated.[39] Similar VT measurements were also performed on **4**$[PF_6]$ (Chart 1), used as reference compound.

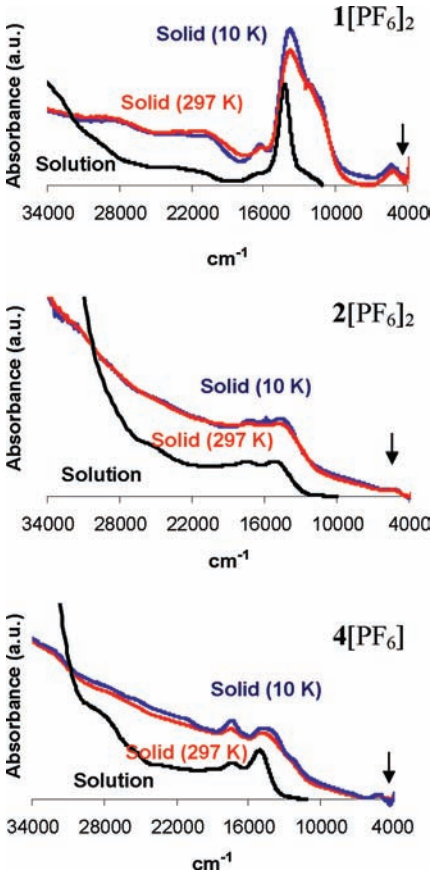

Figure 3. UV−vis−near-IR of the dications of **1**$[PF_6]_2$, **2**$[PF_6]_2$, and **4**$[PF_6]$ in KBr pellets at 10 and 297 K (blue and red lines, respectively) compared to corresponding solution spectra recorded in dichloromethane (black line) at 297 K (peak values for these spectra are given in the Supporting Information). The near-IR transitions of these compounds are indicated by arrows.

The UV−vis spectra obtained at 297 K for these compounds in KBr matrixes resemble those obtained in dichloromethane solutions (Figure 3). Thus, **1**$[PF_6]_2$, **2**$[PF_6]_2$, and **4**$[PF_6]$ are characterized by intense and overlapping bands in the visible range, previously attributed to ligand-to-metal charge-transfer (LMCT) transitions, and by a much weaker absorption in the near-IR range, corresponding to a forbidden d → d transition.[16,17] While the spectra of **1**$[PF_6]_2$ and **2**$[PF_6]_2$ are clearly distinct, an overall similar thermal behavior is observed that resembles that observed for the mononuclear model complex **4**$[PF_6]$. This reversible change principally consists of a very slight increase of the low-energy (LMCT) absorption in the visible range upon a decrease of the temperature to 10 K. Notably, at this temperature, both **1**$[PF_6]_2$ and **2**$[PF_6]_2$ should be quasi-completely present under their singlet and triplet states, respectively. Thus, it is difficult to relate the thermal changes to an increase in the population of a given spin state. These observations, nevertheless, indicate that no large structural changes take place between the different spin states of these compounds.

The IR spectra of these compounds were subsequently examined in KBr between 70 and 400 K (Figure 4). For **2**$[PF_6]_2$ and **4**$[PF_6]$, the spectra obtained at 70 K were virtually identical with those at room temperature, with any shift remaining below the spectral resolution of the

(36) Paul, F.; Toupet, L.; Roisnel, T.; Hamon, P.; Lapinte, C. *Compt. Rend. Chim.* **2005**, *8*, 1174–1185.
(37) Paul, F.; Toupet, L.; Roisnel, T.; Hamon, P.; Lapinte, C. *C. R. Chim.* **2005**, *8*, 1174–1185.
(38) Paul, F.; Toupet, L.; Thépot, J.-Y.; Costuas, K.; Halet, J.-F.; Lapinte, C. *Organometallics* **2005**, *24*, 5464–5478.
(39) Considering a Boltzmann distribution, with a singlet−triplet gap of ca. 380 cm^{-1}, the singlet state of **1**$[PF_6]_2$ should be quite exclusively populated below 70 K (>99.8%), whereas ca. 33% of the corresponding triplet state should be present at ambient temperatures (300 K) and ca. 42% at 380 K.

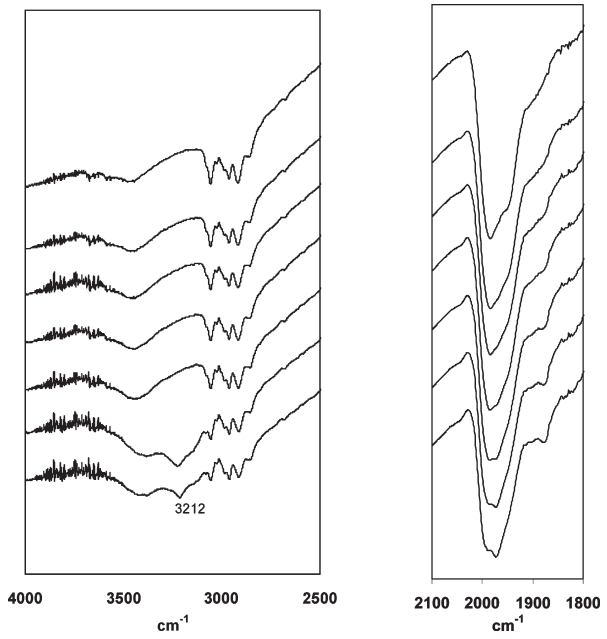

Figure 4. VT-IR spectra of the dication of $\mathbf{1}[PF_6]_2$ in KBr pellets.

spectrometer (± 2 cm^{-1}). In contrast, more significant changes were observed for $\mathbf{1}[PF_6]_2$. Thus, upon a decrease in the temperature, the shoulder on the main peak at 1980 cm^{-1}, near 1970 cm^{-1}, develops into a peak, whereas the former peak becomes a shoulder at 70 K.[39] Decreasing the temperature therefore produces in a slight overall decrease of the most intense $\nu_{C\equiv C}$ stretching mode ($\Delta\nu \approx 10$ cm^{-1}). This shift can be related to the increased cumulenic character observed in the solid-state structure of $\mathbf{1}[PF_6]_2$ at 100 K, in line with a weakening of the $\nu_{C\equiv C}$ stretches in the singlet state relative to the triplet state (Scheme 1b). Also, two new absorptions near 1872 and 3210 cm^{-1} appear at low temperatures. At present, these two weak absorptions could not be assigned to definite vibrational modes. Notably, all of these changes remain reversible with temperature,[39] unless the sample is heated above 380 K.

NMR Characterization of $\mathbf{1}-\mathbf{3}[PF_6]_2$. The ^{1}H and ^{13}C NMR spectra of $\mathbf{1}-\mathbf{3}[PF_6]_2$ have then been recorded at room temperature in dichloromethane-d^2 (Figure 5).[40] The observation of a single set of signals for each compound reveals that the thermal interconversion between the singlet and triplet states of these diradicals takes place faster than the NMR acquisition time, resulting in averaged signals for solutions containing these diradicals under different spin states. Notably, the ^{1}H and ^{13}C NMR signals for $\mathbf{1}[PF_6]_2$ were significantly "sharper" than those obtained for $\mathbf{2}[PF_6]_2$ and $\mathbf{3}[PF_6]_2$, a feature that significantly contributes to the attribution of the various NMR signals detected. However, the most obvious feature of the ^{1}H NMR spectrum of $\mathbf{1}[PF_6]_2$ is that the detected signals are markedly less shifted than those for typical Fe^{III} complexes, such as $\mathbf{4}[PF_6]$ and $\mathbf{5}[PF_6]$ previously studied. For instance, the four equivalent nuclei (H_a) of the arylacetylide bridge of $\mathbf{1}[PF_6]_2$ were observed at -4.6 ppm, whereas the corresponding nuclei (H_a and H_b) of $\mathbf{4}[PF_6]$ showed up either below -41 or above 29 ppm.[29] The unambiguous assignment of all signals of $\mathbf{1}[PF_6]_2$ proved possible using ^{1}H$-^1$H polarization transfer (Supporting Information). The improved resolution of the spectrum also allowed for observation of the nuclear spin$-$spin couplings for the *p*-phenyl protons, providing thereby a means to further confirm the attribution of these nuclei. Thus, the H_3 and H_6 signals of the dppe ligand come out as triplets with a $^3J_{HH}$ of ca. 6.6 and 6.9 Hz, respectively.

The ^{1}H NMR signals for the diradicals $\mathbf{2}[PF_6]_2$ and $\mathbf{3}[PF_6]_2$ were detected in more usual ranges in comparison to $\mathbf{4}[PF_6]$ and $\mathbf{5}[PF_6]$ and were therefore assigned by analogy (Table 3). Thus, rather specific ^{1}H NMR shifts were observed for the "(η^2-dppe)(η^5-C_5Me_5)Fe" fragment. The C_5Me_5 protons (H_9) give each time rise to the most intense peak of the spectrum near -10 ppm, while the *endo*- and *exo*-phenyl protons ($H_1/H_2/H_3$ and $H_4/H_5/H_6$) of the dppe ligand appear in the diamagnetic range as two characteristic sets of signals in a rough 2:2:1 ratio, and the methylene protons (H_7 and H_8) come out slightly above 7 ppm and below 2 ppm, respectively. Among these, only H_8 was detected, with H_7 being presumably hidden below the aromatic dppe protons. As for $\mathbf{4}[PF_6]$ and $\mathbf{5}[PF_6]$, the aromatic protons of $\mathbf{2}[PF_6]_2$ and $\mathbf{3}[PF_6]_2$ correspond to the most shifted signals and were detected at -87.4 ppm (H_a and H_c) and 49.8 ppm (H_b) for $\mathbf{2}[PF_6]_2$ and at -36.8 and 21.9 ppm (H_a and H_b) for $\mathbf{3}[PF_6]_2$. In the case of $\mathbf{2}[PF_6]_2$, the H_a and H_c signals overlap near -87 ppm. This was definitively evidenced by the VT study (Supporting Information) because these signals are differently shifted with temperature. The arylethynyl protons H_a-H_c are much more shifted for $\mathbf{2}[PF_6]_2$ than they are for $\mathbf{4}[PF_6]$ or even for $\mathbf{3}[PF_6]_2$.

Temperature Dependence of the ^{1}H NMR Signals. We have next examined the temperature dependence of the ^{1}H NMR shifts of $\mathbf{1}-\mathbf{3}[PF_6]_2$. For these symmetric dinuclear complexes, this dependence should be similar to that of the corresponding mononuclear Fe^{III} complexes in the case of weak or negligible intramolecular exchange coupling.[41,42] Thus, a $1/T$ dependence converging toward zero for T reaching infinity (Curie behavior) should be observed for the isotropic shift of nuclei remote from the metal center (> 5 Å).[29] However, in the case of a sizable intramolecular coupling, these dinuclear complexes will exist in two nondegenerate spin states (singlet and triplet), with only one among them being paramagnetic (i.e., the triplet state). Depending on the magnitude and nature of the coupling, the population of this paramagnetic state might be significantly modified by any temperature change. Thus, deviations to the Curie behavior might be observed. In such instances, the expected $1/T$ dependence for a fixed concentration of paramagnetic species needs to be corrected for the change in the spin-state population (using a Boltzmann law) to accurately model the

(40) Apart from confirming the proposed structures for $\mathbf{1}[PF_6]_2$, $\mathbf{2}[PF_6]_2$, and $\mathbf{3}[PF_6]_2$, the ^{13}C NMR spectra do not bring any additional information regarding the electronic structure of these species and are therefore reported as Supporting Information along with the proposed assignments for the detected signals.

(41) (a) Bertini, I.; Galas, O.; Luchinat, C.; Parigi, G.; Spina, G. *J. Magn. Reson.* **1998**, *130*, 33–44. (b) Golding, R. M.; Pascual, R. O.; Vrbancich, J. *Mol. Phys.* **1976**, *31*, 731–744.

(42) Bertini, I.; Luchinat, C. *NMR of Paramagnetic Molecules in Biological Systems*; The Benjamin/Cummings Publishing C., Inc.: Menlo Park, CA, 1986.

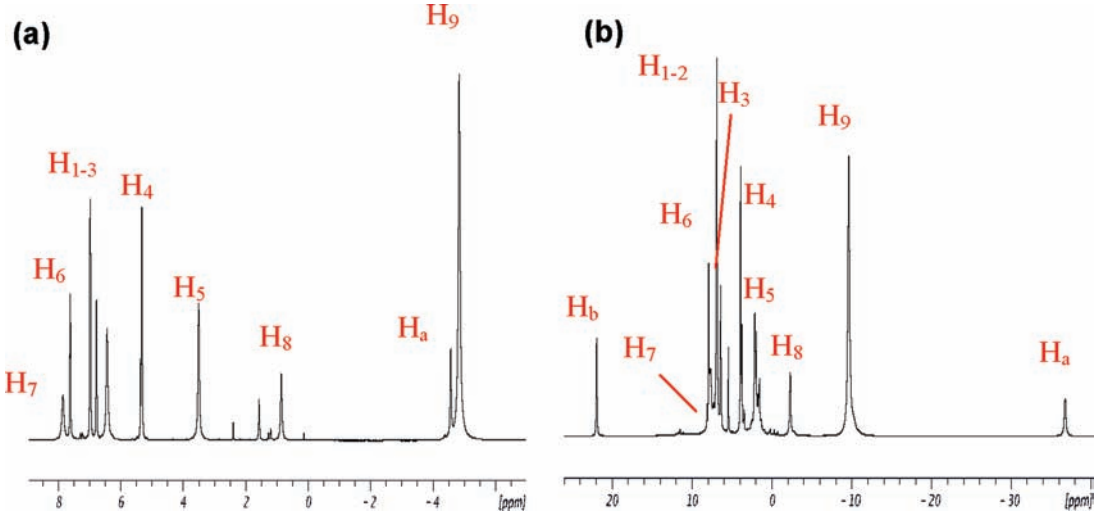

Figure 5. ^{1}H NMR spectra of **1**$[PF_6]_2$ (a) and **3**$[PF_6]_2$ (b) in CD_2Cl_2 at 298 K with proposed assignments for selected protons according to Chart 2.

Chart 2. ^{1}H Nuclei Numeration Corresponding to the Proposed Assignments for **1**−**5**$[PF_6]$

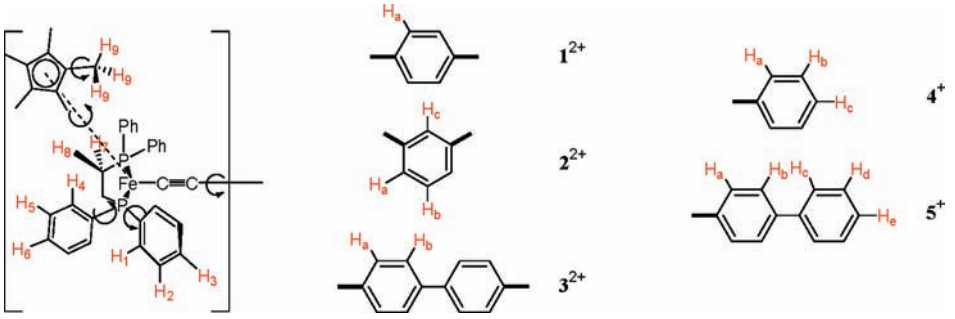

^{1}H NMR shifts. Accordingly,[28] the isotropic shifts of strongly exchange-coupled systems for which the entropy can be reduced to its electronic term follow eq 3 rather than a typical Curie law, as previously observed for organic[43] or inorganic[44] diradicals featuring magnetically coupled doublets ($S = {}^1/_2$). In this equation, δ_{iso}, which stands for the paramagnetic shift (in ppm), is proportional to the Boltzmann population of the triplet state, while *a* and *b* stand for adjustable fitting parameters.

$$\delta_{iso} = a\frac{1}{3+\exp\left(-\frac{2J_{ab}}{kT}\right)} + b \qquad (3)$$

This behavior is precisely what is stated for the ^{1}H NMR isotropic shifts of **1**$[PF_6]_2$ between 300 and 180 K (Figure 6a). The temperature dependence of the most shifted ^{1}H NMR signals such as those of the aromatic protons (H_a), of the C_5Me_5 protons (H_9), and of the *exo*-methylene protons of dppe (H_8) could be fitted using eq 3. By this means, J_{ab} values around -170 ± 2 and -171 ± 3 cm^{-1}, in good agreement with the solid-state value obtained by SQUID measurements (191 ± 3 cm^{-1}), were found for **1**$[PF_6]_2$ in a dichloromethane-d^2 or acetone-d^6 solution, respectively. The extrapolated shifts at 0 K (singlet state) fall ca. 3 ppm above those of the parent Fe^{II} diamagnetic complex **1**. Such slight deviations to "ideal" values were, however, expected because eq 3 applies only to isotropic shifts taken as pure contact shifts, whereas a small pseudocontact contribution was previously demonstrated for the signals presently fitted (H_a, H_8, and H_9).[29] Note that the significantly lower ^{1}H and ^{13}C NMR shifts exhibited by that compound at 298 K relative to those of **4**$[PF_6]$ already pointed toward the existence of a strong antiferromagnetic interaction for this organometallic Fe^{III} diradical.

For corresponding protons of **2**$[PF_6]_2$, in spite of the strong ferromagnetic coupling evidenced by SQUID measurements, an apparently linear plot against $1/T$ was obtained with very good regression coefficients ($R^2 > 98\%$) in the same temperature range (Figure 6b). While perhaps surprising at first sight in comparison to the plot previously obtained for **1**$[PF_6]_2$, this Curie dependence of the isotropic shifts was actually expected. Indeed, given the very large ferromagnetic J_{ab} coupling ($+150$ cm^{-1}) measured for this diradical, it behaves as a quasi-pure triplet state in the temperature range investigated because only a small change in the triplet population (ca. 4%) takes place between 300 and 180 K. The latter cannot induce any detectable curvature of the δ vs $1/T$ plot with regard to the experimental uncertainties on the shifts (± 0.3 ppm).[45,46]

Finally, **3**$[PF_6]_2$ also exhibits a perfect Curie behavior in dichloromethane-d^2 (Figure 6c). Again, such a linear dependence on $1/T$ indicates a fairly constant concentration of the paramagnetic Fe^{III} species over the temperature range investigated. This time, in line with the

(43) Kopf, P.; Kreilick, R. *J. Am. Chem. Soc.* **1969**, *91*, 6569–6573.
(44) Kriley, C. E.; Fanwick, P. E.; Rothwell, I. P. *J. Am. Chem. Soc.* **1994**, *116*, 5225–5232.

Table 1. Detected (δ) and Isotropic (δ_{iso}) ^{1}H NMR Shifts Recorded for **1**−**5**$[PF_6]_2$ and Extrapolated Isotropic Shifts $(\delta_{iso})_T$ for **1**−**3**$[PF_6]_2$ in the Triplet State at 298 K in CD_2Cl_2[a]

		−C≡C−Ar					dppe								C_5Me_5
compd	δ (ppm)	H_a	H_b	H_c	H_d	H_e	H_1	H_2	H_3	H_4	H_5	H_6	H_7	H_8	H_9
$\mathbf{1}^{2+}$	δ	−4.5					6.4	7.0	6.8	3.4	5.3	7.6	7.8	0.8	−4.9
	δ_{iso}[b]	−11.7					−1.7	−0.2	−0.4	−3.9	−1.8	0.4	5.0	−1.1	−6.4
	$(\delta_{iso})_T$[c]	−34.8					−5.1	−0.6	−1.2	−11.6	−5.4	1.2	14.9	−3.3	−19.0
$\mathbf{2}^{2+}$	δ	−87.4	49.8	−87.4			6.5	6.9	6.2	1.6	3.6	8.0	n.d.	−2.9	−10.8
	δ_{iso}[b]	−94.6	42.6	−94.3			−1.6	−0.3	−1	−5.7	−3.5	0.8	n.d.	−4.8	−12.3
	$(\delta_{iso})_T$[c]	−101.3	45.6	−101.0			−1.7	−0.3	−1.1	−6.1	−3.7	0.9	n.d.	−5.1	−13.2
$\mathbf{3}^{2+}$	δ	−36.8	21.9				6.9	6.9	6.4	2.0	3.9	7.9	7.7[d]	−2.3	−9.7
	δ_{iso}[b]	−44.1	15.1				−1	−0.4	−0.9	−5.3	−3.4	0.6	5.0	−4.3	−11.4
	$(\delta_{iso})_T$[c]	−58.8	20.1				−1.3	−0.5	−1.2	−7.1	−4.5	0.8	6.7	−5.7	−15.2
$\mathbf{4}^{+d}$	δ	−41.7	29.2	−41.7			nd	6.8	6.2	1.8	3.7	7.9	n.d.	−2.8	−10.5
	δ_{iso}	−48.9	22.0	−48.8			nd	−0.4	−1.1	−5.5	−3.5	0.3	4.8	−4.6	−11.9
$\mathbf{5}^{+d}$	δ	−44.8	30.9	−0.4[d]	11.8	−0.8[d]	nd	6.8	6.3	1.6	3.7	8.0	n.d.	−2.8	−10.3
	δ_{iso}	−51.6	23.5	−7.8	3.8	−8.0	−0.6	−0.6	−1.1	−5.8	−3.7	0.6	n.d.	−4.8	−11.7

[a] Proposed attribution according to Chart 2 ($CHDCl_2$ at 5.35 ppm, $\delta \pm 0.2$ ppm); "nd" and "n.d." both stand for "not detected". [b] This isotropic shift corresponds to the fraction of the triplet dinuclear Fe^{III} compound present in solution at 298 K. [c] Isotropic shift derived for the "pure" triplet diradical at 298 K; $(\delta_{iso})_T = \delta_{iso}/P_T$. [d] Tentative assignment.[29]

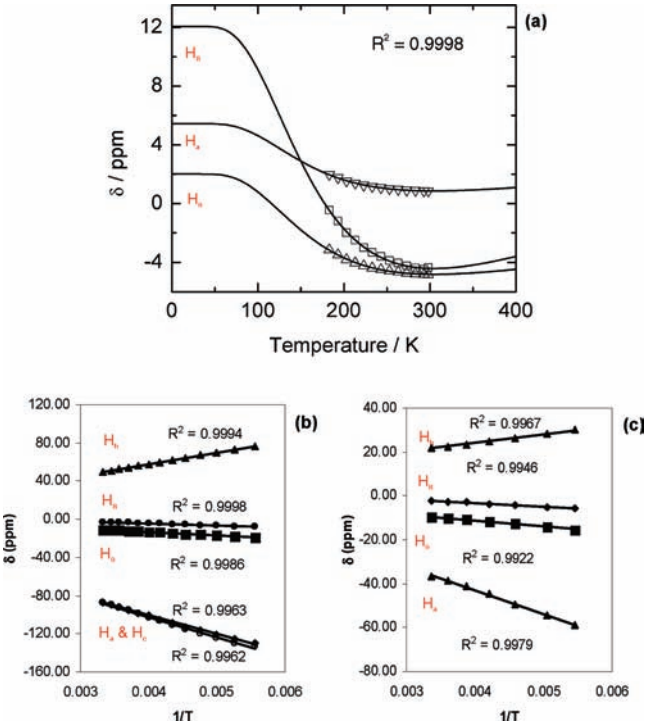

Figure 6. Temperature dependence of selected ^{1}H NMR shifts for **1**$[PF_6]_2$ (a), **2**$[PF_6]_2$ (b), and **3**$[PF_6]_2$ (c) in CD_2Cl_2 with proposed assignments according to Chart 2 and corresponding fits (see the text).

solid-state SQUID measurements,[48] the Curie dependence evidences a very weak intramolecular exchange coupling. Indeed, an exchange coupling such as that measured in the solid state for this compound (≈ -1 cm^{-1}) should not induce any detectable change from the statistical population of the triplet state between 310 and 190 K for **3**$[PF_6]$.

Derivation of Hyperfine Coupling Constants and Spin Densities for Selected *C*H Carbon Atoms of the Bridge of 1−**3**$[PF_6]_2$**.** Similar to what had been previously done for $S = {}^1/_2$ mononuclear Fe^{III} radical cations such as **4**$[PF_6]$ and **5**$[PF_6]$,[29] the ^{1}H NMR shifts of **1**−**3**$[PF_6]_2$ were used to derive the proton isotropic hyperfine coupling constants (A_H) as well as the atomic spin densities $(\rho^\pi)_C$ in the π manifold for the carbon atoms of the bridging ligand that carry a proton. This is interesting because these data

Table 2. Isotropic Hyperfine Coupling Constants for Selected Protons of **1**−**5**$[PF_6]_2$ at 295 K and π-Spin Densities on the Neighboring Carbon Derived from This Quantity

		bridging aryl(s)					C_5Me_5
compd		H_a	H_b	H_c	H_d	H_e	H_9
1$[PF_6]_2$	A_H[a]	−0.15					−0.08
	$\rho_{C(H)}$[b]	0.016					
2$[PF_6]_2$	A_H[a]	−0.44	0.20	−0.44			−0.06
	$\rho_{C(H)}$[b]	0.042	−0.017	0.043			
3$[PF_6]_2$	A_H[a]	−0.26	0.09				−0.07
	$\rho_{C(H)}$[b]	0.025	−0.007				
4$[PF_6]$	A_H[a]	−0.57	0.26	−0.57			−0.14
	$\rho_{C(H)}$[b]	0.028	−0.011	0.027			
5$[PF_6]$	A_H[a]	−0.60	0.27	−0.09	0.04	−0.09	−0.14
	$\rho_{C(H)}$[b]	0.029	−0.012	0.004	−0.001	0.004[c]	

[a] Hyperfine coupling constants (G) for selected protons (obtained with the g value of the corresponding monomer model, i.e., **4**$[PF_6]$ or **5**$[PF_6]$). [b] π-Spin (e) densities on the neighboring carbon derived using the McConnell relationship (eq 5). [c] Tentative value (i.e., based on a tentative assignment).

(45) Attempts to fit the VT data using eq 3 reveal a poor sensitivity of the fitting procedure to J_{ab}, in contrast to what had been observed for **1**$[PF_6]_2$. Data exhibiting a clear curvature above the experimental uncertainty in the probed temperature range are required for extracting a unique and sensible (a, b, J_{ab}) set by fitting of the data with eq 3.[46] The ferromagnetic coupling of **2**$[PF_6]_2$ is obviously too strong for that between 300 and 180 K, while the solubility and high sensitivity of this diradical precluded us to explore higher temperatures than 300 K. Actually, it is a well-known fact that extracting J_{ab} values from VT studies constitutes a more challenging task for ferromagnetically exchange-coupled diradicals than for antiferromagnetically coupled ones.[27,47]

(46) Paul, F.; Cador, O. Work in progress.

(47) Platz, M. S. In *Diradicals*; Borden, W. T., Ed.; Wiley-Interscience: New York, 1982; pp 195−258.

(48) Moreover, the facile rotation around the central bond of the biphenyl unit in solution also certainly contributes to the further reduction of the magnitude of the intramolecular exchange coupling relative to that in the solid state. Indeed, according to previous studies on biphenyl-bridged diradicals,[49] the quasi-planar conformation of the biphenyl unit previously evidenced in the solid state[17] should be optimal for transmitting any antiferromagnetic interaction.

Table 3. Calculated Spin Densities (in electrons) on Selected Fragments or Atoms for $\{(dpe)(\eta^5\text{-}C_5H_5)Fe(C{\equiv}C)\}_2(Ar)$ Complexes (**1**-H^{2+}, **2**-H^{2+}, and **3**-H^{2+}) under the T or BS State [Atom Numbering According to Chart 3; Ar = 1,4-C_6H_4 (a); 1,3-C_6H_4 (b); 4,4′-$C_{12}H_8$ (c)]

		C_5H_5	dpe		C_5H_5'	dpe′	C≡C(C_6H_4)								ΔE [a] (cm^{-1})
compd	Fe	C [b]	P [b]	Fe′	C′ [b]	P′ [b]	C_a	C_b	C_a'	C_b'	C_c	C_d	C_e	C_f	
1-H^{2+} (T)	1.000	−0.018	−0.030	1.009	−0.018	−0.030	−0.088	0.190	−0.086	0.188	0.007 [c]	0.022 [c]			510
1-H^{2+} (BS)	0.952	−0.017	−0.028	−0.948	0.012	0.028	−0.147	0.228	0.146	−0.228	−0.113 [d]	0.092 [d]			
2-H^{2+} (T)	0.984	−0.017	−0.028	0.984	−0.017	−0.028	−0.121	0.219	−0.121	0.219	−0.071 [c]	0.120	−0.071	0.120 [c]	512
2-H^{2+} (BS)	0.990	−0.017	−0.029	−0.990	0.018	0.028	−0.103	0.204	0.102	−0.207	−0.017 [d]	0.001	−0.006	0.000 [d]	
3-H^{2+} (T)	0.933	−0.016	−0.026	0.934	−0.016	−0.027	−0.091	0.213	−0.091	0.213	−0.033 [c]	0.055 [c]	−0.022 [c]	0.059 [c]	158
3-H^{2+} (BS)	0.916	−0.016	−0.026	−0.914	0.016	0.026	−0.102	0.220	0.102	−0.220	−0.060 [d]	0.072 [d]	−0.051 [d]	0.088 [d]	
4-H^{+} [e]	0.871	−0.014	−0.024				−0.074	0.223			−0.038	0.072	−0.040	0.092	
5-H^{+} [e]	0.780	−0.012	−0.020				−0.044	0.211			−0.029/ −0.014 [f]	0.070/ 0.025 [f]	−0.038/ −0.013 [f]	0.098/ 0.031 [f]	

[a] The spin densities of the carbon and phosphorus atoms of respectively the C_5H_5 and dpe ligands are averaged. [b] J_{ab} computed according to eq 7 (cm^{-1}). [c] Average value between chemically equivalent nuclei. [d] Same value of opposite sign for C_x'. [e] Computed for the perpendicular conformation of the aryl ring linked to the acetylide spacer. [29] [f] C_c/C_g, C_d/C_h, C_e/C_i, and C_f/C_j indicated for **5**-H^{+}.

Chart 3. Labels of the Model Compounds **1**-H^{2+}, **2**-H^{2+} and **3**-H^{2+} used in the DFT Computations

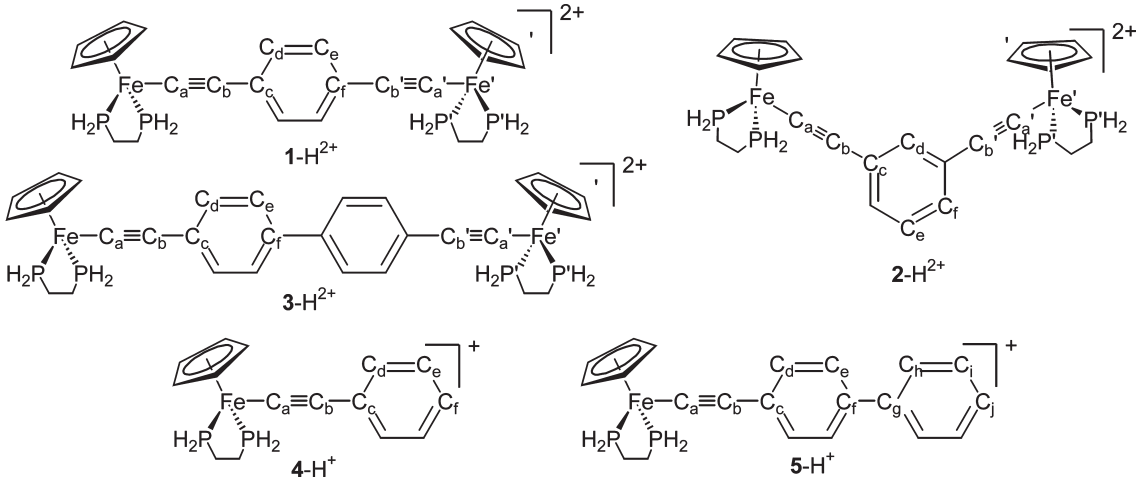

provide important experimental insight regarding the spin distribution within these organometallic diradicals. These data cannot be obtained from ESR measurements because of the fast electronic relaxation of these compounds.[11,17]

As previously discussed (eq 4a), the NMR shift (δ) of a paramagnetic compound is the sum of a diamagnetic contribution (δ_{dia}) and of an isotropic contribution (δ_{iso}), which actually originates from the presence of the electronic spin of the unpaired electron(s).[42] The latter contribution (eq 4b) is itself the sum of a contact (δ_c) and pseudocontact term (δ_{pc}), with the contact term being proportional to the local atomic spin density (Supporting Information).

$$\delta = \delta_{dia} + \delta_{iso} \quad (4a)$$

$$\delta_{iso} = \delta_c + \delta_{pc} \quad (4b)$$

$$\delta = \delta_{dia} + P_T(\delta_{iso})_T \quad (4c)$$

$$P_T = \frac{3}{3 + \exp(-\frac{2J_{ab}}{kT})} \quad (4d)$$

However, for exchange-coupled Fe^{III} diradicals possessing spin states in rapid interconversion, such as **1**−**3**-$[PF_6]_2$, the situation is slightly more complex than that for Fe^{III} monoradicals because the isotropic shift computed using eq 4b originates only from the fraction of the diradical in the (paramagnetic) triplet state and not from the totality of diradicals present in solution, with the singlet state being presumed to exhibit the same NMR shifts as the neutral Fe^{II} parent of **1**. The observed NMR shift is therefore the sum of a diamagnetic contribution and of what we could call an "apparent" isotropic contribution (eq 4c). Indeed, a simple analysis (see the Supporting Information) reveals that this "apparent" contribution actually corresponds to the hypothetical isotropic shift $(\delta_{iso})_T$ that a given diradical in its "pure" triplet state would exhibit, multiplied by the partition function P_T (eq 4d) of the triplet state at the temperature of the NMR measurement.[26] Isotropic shifts of the "pure" triplet diradical at ambient temperatures $(\delta_{iso})_T$, which are actually the quantities required to derive spin densities for the paramagnetic state of the diradical, can thus be simply obtained by dividing the isotropic shift (δ_{iso}) of a given proton by the partition function of the triplet state at 298 K (Tables 3 and 4).[50] These isotropic shifts of the triplet state [$(\delta_{iso})_T$; Table 3] were thus

(49) (a) McConnell, H. M. *J. Chem. Phys.* **1960**, *33*, 1868–1869. (b) McConnell, H. M. *J. Chem. Phys.* **1960**, *33*, 115–121.

(50) For example, ca. 33% for **1**$[PF_6]_2$, 93% for **2**$[PF_6]_2$, and 75% for **3**$[PF_6]_2$.

Table 4. Crystal Data, Data Collection, and Refinement Parameters for $\mathbf{1}[PF_6]_2 \cdot CH_2Cl_2$

	100(1) K	293(2) K
formula	$Fe_2P_4C_{82}H_{82} \cdot 2PF_6 \cdot CH_2Cl_2$	
fw	1677.92	
cryst syst	monoclinic	
space group	$P2_1/c$	
a (Å)	12.9884(3)	13.1083(5)
b (Å)	19.6249(5)	19.9390(6)
c (Å)	29.3740(8)	29.6231(9)
α (deg)	90.00	90.00
β (deg)	92.145(2)	92.210(3)
γ (deg)	90.00	90.00
V (Å^3)	7482.1(3)	7736.7(4)
Z	4	
D(calcd) (g cm^{-3})	1.490	1.441
cryst size (mm)	0.22 × 0.20 × 0.15	
F(000)	3464	
radiation	Mo Kα	
abs coeff (mm^{-1})	0.664	0.642
data collection: θ_{max} (deg), Ω rotation (deg), seconds/frame	54, 0.7, 20	
Θ range	2.76−29.91	2.73−32.29
h, k, l	−15/18, −27/21, −40/41	−18/18, −19/29, −41/42
no. of total reflns	60 939	66 973
no. of unique reflns	19 371	23 909
no. of obs reflns [$I > 2\sigma(I)$]	12 671	9165
restraints/param	0/937	0/937
$w = 1/[\sigma^2(F_o)^2 + (aP)^2 + bP]$ (where $P = [F_o^2 + 2F_c^2]/3$)	$a = 0.0873$, $b = 0.0000$	$a = 0.1459$, $b = 0.0000$
final R	0.049	0.052
R_w	0.139	0.147
R indices (all data)	0.084	0.144
R_w (all data)	0.149	0.176
GOF/F^2 (S_w)	1.050	0.611
$\Delta\rho_{max}$ (e Å^{-3})	1.747	0.606
$\Delta\rho_{min}$ (e Å^{-3})	−1.781	−0.476

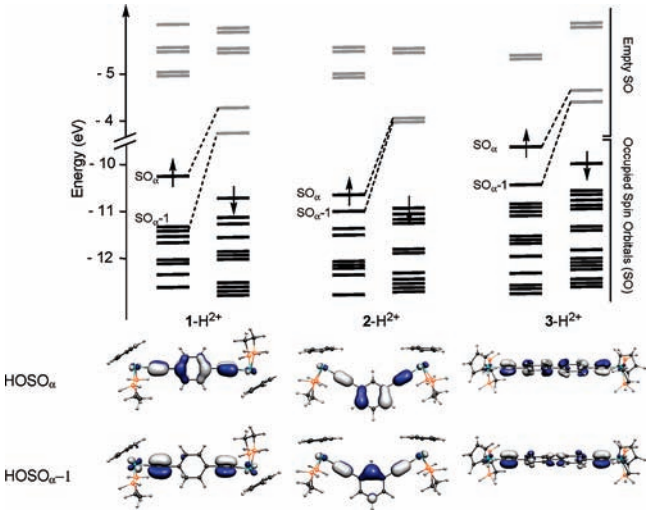

Figure 7. Energy diagram of the frontier spin orbitals of the optimized systems **1**-H^{2+}, **2**-H^{2+}, and **3**-H^{2+} in their triplet spin states. The two highest-occupied α-spin orbitals are plotted (isocontour 0.05 [e bohr^{-3}]$^{1/2}$).

determined for the aromatic protons of the arylacetylide spacer of $\mathbf{1}-\mathbf{3}[PF_6]_2$.

$$A_H = (\delta_{iso})_T \hbar \times 3\gamma_H kT/[g\mu_B S(S+1)] \qquad (5)$$

Values of the hyperfine coupling constants (A_H) for the corresponding protons were next derived using eq 5,[51,52] as was previously done for $\mathbf{4}[PF_6]$ or $\mathbf{5}[PF_6]$.[29] In this equation, γ_H is the proton magnetogyric ratio, μ_B is the Bohr magneton, k is the Boltzmann constant, $\hbar$ is the reduced Planck constant, g is the electron g value, and S is the spin of the diradical. Unlike what happens for organic radicals, A_H values for inorganic complexes are not proportional to the corresponding atomic spin densities because of the pseudocontact contribution to $(\delta_{iso})_T$ from the spin density located on the nearby metal center. Some A_H values are, nevertheless, given for selected protons remote from the metal center in Table 2.

$$(A_H)_c = (\delta_c)_T \hbar \times 3\gamma_H kT/[g\mu_B S(S+1)] \qquad (6a)$$

$$(A_H)_c/h = (Q_{CH})^H (\rho^\pi)_C/2S \qquad (6b)$$

However, when contact shifts of the pure triplet state [$(\delta_c)_T$; see Supporting Information] are used instead of the isotropic shifts in eq 5, "contact" proton hyperfine coupling constants are obtained [$(A_H)_c$; eq 6a]. These constants are now proportional to the spin density present on the corresponding protons. From these $(A_H)_c$ values, the spin density $(\rho^\pi)_C$ present in the π manifold on the nearby carbon atom can then be deduced using the McConnell equation (eq 6b). In this equation, $(A_H)_c/h$ values were expressed in megahertz and $(Q_{CH})^H$ is a constant presently taken as −66 MHz.[42,53] As was previously

(51) Bertini, I.; Luchinat, C.; Parigi, G. *Solution NMR of Paramagnetic Molecules. Application to Metallobiomolecules and Models*; Elsevier: Amsterdam, The Netherlands, 2001.

(52) (a) McConnell, H. M.; Chesnut, D. B. *J. Chem. Phys.* **1958**, *27*, 984–985. (b) McConnell, H. M.; Chesnut, D. B. *J. Chem. Phys.* **1958**, *28*, 107–117. (c) McConnell, H. A. *J. Chem. Phys.* **1958**, *28*, 1188–1192.

(53) For the aromatic protons of the bridging ligands in $\mathbf{1}[PF_6]_2$, $\mathbf{2}[PF_6]_2$, and $\mathbf{3}[PF_6]_2$, we have checked that when the hyperfine constants (A_H) are directly used in eq 6b, very close values for the corresponding spin densities can be obtained (Supporting Information). This amounts to neglect of the pseudocontact contribution from metal center to these values.

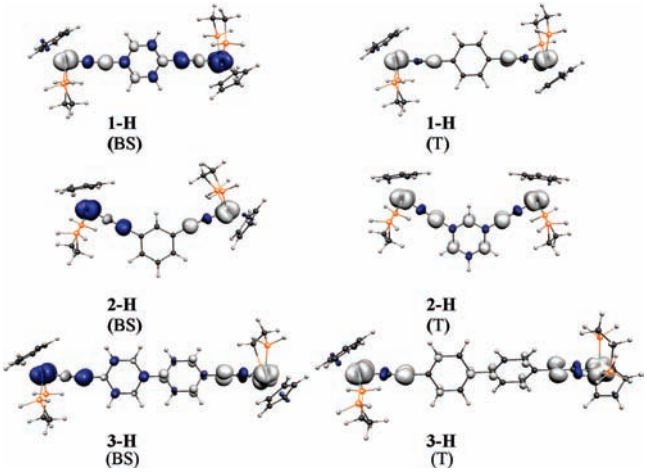

Figure 8. Plots of the total spin densities for $\{(\eta^2\text{-dpe})(\eta^5\text{-}C_5H_5)Fe\text{-}(C{\equiv}C)\}_2(Ar)$ complexes (**1**-H^{2+}, **2**-H^{2+}, and **3**-H^{2+}) in the T and BS States. The contour values are ±0.005 [e $bohr^{-3}$].

discussed,[29] such an approach will be correct only for radicals possessing an axial or pseudoaxial symmetry (i.e., with a slight rhombic deformation) of their *g* tensors and negligible nonlocal dipolar effects on the ^{1}H NMR isotropic shifts. An additional assumption for dinuclear Fe^{III} complexes is that the zero-field-splitting effects are negligible.[54] These assumptions are overall sensible and should lead to fair estimates for the spin densities on the primary carbon atoms of the bridging ligand (Table 2).

DFT Computations on Model Compounds 1-H^{2+}, 2-H^{2+}, and 3-H^{2+}. DFT investigations were performed on the dinuclear Fe^{III} model complexes **1**-H^{2+}, **2**-H^{2+}, and **3**-H^{2+} and on the mononuclear models **4**-H^+ and **5**-H^+ [with the extension "-H" meaning that dppe and C_5Me_5 ligands have been replaced by 1,2-diphosphinoethane (dpe) and C_5H_5, respectively, in $\mathbf{1}^{2+}$, $\mathbf{2}^{2+}$, $\mathbf{3}^{2+}$, $\mathbf{4}^+$, and $\mathbf{5}^+$]. The dinuclear complexes **1**-H^{2+}, **2**-H^{2+}, and **3**-H^{2+} were optimized in their broken-symmetry singlet (BS) and triplet (T) spin states without any symmetry constraint (see the Computational Details section). It has to be noted that the singlet closed-shell states were calculated much higher in energy than the T and BS states in all cases (> 1 eV) and were thus not considered thereafter. The bond lengths and angles around the metal centers in **1**-H^{2+} and **3**-H^{2+} are in good agreement with the X-ray structures available for $\mathbf{1}[PF_6]_2\cdot CH_2Cl_2$ and $\mathbf{3}[PF_6]_2\cdot 2CH_2Cl_2$[17] (see the Supporting Information). The conformations of the arylethynyl ring and the metallic end groups in **1**-H^{2+} and **3**-H^{2+}, calculated in vacuum, are different from those found in the solid-state experimental structures.[55] The mononuclear complexes **4**-H^+ and **5**-H^+ were also investigated for the sake of comparison.

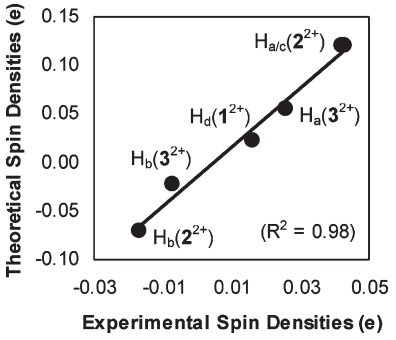

Figure 9. Spin densities determined by ^{1}H NMR for selected carbon atoms of the bridge for **1**−**3**$[PF_6]_2$ versus spin densities computed for the same atoms by DFT for **1**-H^{2+}, **2**-H^{2+}, and **3**-H^{2+}.

The spin contamination of the triplet (T) states of **1**-H^{2+}, **2**-H^{2+}, and **3**-H^{2+} is negligible ($\langle\hat{S}^2\rangle$ = 2.05, 2.07, and 2.08 for **1**-H^{2+}, **2**-H^{2+}, and **3**-H^{2+}, respectively). On the contrary, the BS state is by definition not a pure singlet spin state and contains a large admixture of the triplet wave function ($\langle\hat{S}^2\rangle$ = 0.79, 0.65, and 0.75 for **1**-H^{2+}, **2**-H^{2+}, and **3**-H^{2+}, respectively).[56] The energy diagrams of **1**-H^{2+}, **2**-H^{2+}, and **3**-H^{2+} in their triplet states are given in Figure 7. Their frontier spin orbitals show a large metallic and acetylide character (see Figure 7), as was found previously in studies on similar or closely related compounds.[9,16,29] It has to be emphasized that the nodal properties of the frontier spin orbitals of **1**-H^{2+} and **3**-H^{2+} are really similar to those calculated for the mononuclear Fe^{III} species, **4**-H^+ and **5**-H^+.[29] The atomic spin densities are given in Table 3 for all studied compounds in their T and BS spin states.

$$2J_{ab} = E^{BS} - E^{T} \quad (7)$$

The magnetic couplings in **1**-H^{2+}, **2**-H^{2+}, and **3**-H^{2+} have then been evaluated using eq 7, independently proposed by Yamaguchi et al.[58] and by Ruiz et al.[33,59] (see Table 3). Antiferromagnetic interactions of −255 and −79 cm^{-1} were calculated for **1**-H^{2+} and **3**-H^{2+}, respectively, while a ferromagnetic interaction of +256 cm^{-1} was found for **2**-H^{2+}.

Discussion

The present investigation provides a better picture of the electronic structures of **1**−**3**$[PF_6]_2$. We will now discuss step-by-step every point made by this work before coming to the magnetic properties of these organometallic Fe^{III} diradicals in connection with geometrical/structural issues.

Spin Distribution in the Triplet States of 1−3$[PF_6]_2$. ^{1}H NMR allowed for the derivation of isotropic hyperfine couplings (A_H) for selected protons of **1**−**3**$[PF_6]_2$

(54) (a) Wicholas, M.; Mustacich, R.; Jayne, D. *J. Am. Chem. Soc.* **1972**, *94*, 4518–4522. (b) La Mar, G. N.; Eaton, G. R.; Holm, R. H.; Walker, F. A. *J. Am. Chem. Soc.* **1973**, *95*, 63–75.

(55) A complete study of the potential energy surface associated with the geometrical parameters of these compounds was not possible because of an unaffordable computational cost, but several starting conformations of the metallic end groups $(\eta^2\text{-dpe})(\eta^5\text{-}C_5H_5)Fe$ relative to the bridging ligand were considered. Even though our conformational study was not exhaustive, each system always reorganized itself into to a unique geometry regardless of the starting geometry considered. It has to be noted that NMR indicates the fluxionality of the metallic end groups in solution.

(56) The BS states are useful for energetic considerations.[57] Given that their geometries do not correspond to those of the authentic singlet states, more pronounced differences can be expected between the structural arrangement of the triplet and the "true" singlet states.

(57) (a) Noodleman, L. *Chem. Phys.* **1986**, *109*, 131. (b) Noodleman, L. *J. Chem. Phys.* **1981**, *74*, 5737–5743.

(58) (a) Nishino, M.; Yamanaka, S.; Yoshioka, Y.; Yamaguchi, K. *J. Phys. Chem. A* **1997**, *101*, 705–712. (b) Yamaguchi, K.; Fukui, H.; Fueno, T. *Chem. Lett.* **1986**, 625–628.

(59) Ruiz, E.; Alvarez, S.; Cano, J.; Polo, V. *J. Chem. Phys.* **2006**, *124*, 107102.

(Table 2). Although the values for C_5Me_5 protons contain a potentially sizable pseudocontact contribution,[29] a comparison between the values found for the pentamethylcyclopentadienyl protons and those for the most shifted protons of the arylethynyl linker (Table 2) suggests that a significantly larger spin density is present on the bridging arylethynyl ligand in these diradicals.[60] The DFT computations on **1**-H^{2+}, **2**-H^{2+}, and **3**-H^{2+} substantiate this picture by evidencing that the spin density for the paramagnetic diradicals is strongly located on the metal centers (Figure 8). Furthermore, the spin density on the organometallic (η^2-dpe)(η^5-C_5H_5)Fe fragments remains roughly constant for **1**-H^{2+}, **2**-H^{2+}, and **3**-H^{2+} in the triplet state (Table 3), in spite of the different central spacers present in these three diradicals. In line with these calculations, the relative constancy of the extrapolated $(\delta_{iso})_T$ values for the dppe and C_5Me_5 protons and carbon atoms of **1**−**3**$[PF_6]_2$ at ambient temperature (Table 3 and Supporting Information) reveals that a similar statement certainly holds for the "(η^2-dppe)(η^5-C_5Me_5)Fe" fragments in these compounds.

In contrast to what precedes, large differences in the spin distribution take place between corresponding aromatic carbon atoms of the bridging ligands in **1**−**3**$[PF_6]_2$, as evidenced by the markedly different A_H values found (Table 2). For instance, compared to **3**$[PF_6]_2$, NMR reveals that the spin density on each *o*-carbon atom is roughly twice as important in **2**$[PF_6]_2$ and halved in **1**$[PF_6]_2$. As was anticipated, the atom-by-atom spin alternation previously observed for the arylethynyl ligand in Fe^{III} monoradicals can hardly be preserved in the short *p*-phenylene bridge of **1**$[PF_6]_2$ for obvious symmetry reasons. According to NMR, only a positive spin density is present on the bridging aromatic unit of **1**$[PF_6]_2$ in the triplet state. In contrast, NMR reveals that spin alternation is still present on the phenylene rings of the bridge in the triplet state of **2**$[PF_6]_2$ and **3**$[PF_6]_2$ (Table 2). These features are well reproduced by the DFT computations (Figure 8 and Table 3), and actually a good linear correlation (R^2 = 0.98) is found between the spin densities computed for these carbon atoms in **1**-H^{2+} to **2**-H^{2+} and **3**-H^{2+} in the triplet state and those experimentally determined for **1**−**3**$[PF_6]_2$ (Figure 9).[61] The nonunity slope of the fit (3.0) reveals, however, that spin delocalization is somewhat overestimated by DFT in comparison to that determined by ^{1}H NMR, a statement already made previously.[29,62]

Comparison between the Paramagnetic Dinuclear and Corresponding Mononuclear Fe^{III} Compounds. The DFT computations on **1**-H^{2+}, **2**-H^{2+}, **3**-H^{2}, **4**-H^{+}, and **5**-H^{+} also indicate that the geometry within each "(η^2-dpe)-(η^5-C_5H_5)Fe" fragment remains very close in the dinuclear and mononuclear complexes, with a slight decrease regarding the spin density delocalized on the Fe^{III} centers being stated for the mononuclear complexes. Further, the highest-occupied spin orbital of the triplet states of **1**-H^{2+} and **3**-H^{2+} closely resembles those of the corresponding mononuclear Fe^{III} radicals **4**-H^{+} and **5**-H^{+}, suggesting that the magnetic coupling does only induce a small perturbation of the electronic structure of the spin-carrying units in the dinuclear Fe^{III} complexes relative to the mononuclear ones.

Under such circumstances, Bertini and co-workers have shown that the isotropic NMR shifts exhibited by polynuclear paramagnetic assemblies are related to those of the corresponding mononuclear (model) complexes at any temperature.[51] On the basis of their work, eq 8 can be derived (Supporting Information). This equation, which relates the apparent ^{1}H NMR isotropic shifts of dinuclear compounds to those of the corresponding mononuclear models, provides therefore a convenient experimental means to check if any detectable changes are induced by the magnetic exchange coupling in the electronic structure of the interacting organoiron fragments. In this equation, the summation ($\sum_x$) takes place over the paramagnetic Fe^{III} centers "sensed" by a given nucleus belonging to the inorganic triplet diradical, where $(\delta_{iso})_D$ represents the apparent isotropic shift of this nucleus for this diradical (i.e., δ_{iso} in Table 1), $(\delta_{iso})_{Mx}$ stands for the isotropic shift of the same nucleus in the corresponding (doublet) mononuclear complex used as a reference, and P_T is the partition coefficient of the triplet state (eq 4d). This equation has often been used with weakly coupled organic diradicals (P_T = $^3/_4$), in which case an even simpler expression results.[25]

$$(\delta_{iso})_D = \frac{4}{3}[\sum_x (\delta_{iso})_{Mx}]P_T \qquad (8)$$

It can be easily stated that the ^{1}H NMR isotropic shifts of the dppe and C_5Me_5 ligands for **1**$[PF_6]_2$, **2**$[PF_6]_2$, and **4**$[PF_6]$ and those of **3**$[PF_6]_2$ and **5**$[PF_6]$ (Table 1) reasonably conform to eq 8. An excellent match cannot be expected for these poorly shifted signals, which only "sense" the electronic spin located on the nearby metal center. However, regarding the more shifted protons of the carbon-rich bridge, which sense the spin density located on the two Fe^{III} centers, things are more contrasted. Indeed, a satisfactory agreement with eq 8 is obtained for protons of **1**$[PF_6]_2$ and **3**$[PF_6]_2$, but significant deviations are stated for **2**$[PF_6]_2$. Thus, an apparent isotropic shift of −12.1 ppm is predicted for the four equivalent H_a protons (Chart 2) in **1**$[PF_6]_2$, using the isotropic shifts recorded for H_a and H_b in **4**$[PF_6]$, to compare with the experimental shift of −11.7 ppm. The apparent ^{1}H NMR isotropic shifts of H_a or H_b of **3**$[PF_6]_2$ (−44.1 and 15.1 ppm, respectively) are also fairly well approached by respectively summing the shifts of H_a and H_d and of H_b and H_c for **5**$[PF_6]$ (−47.8 and 15.5 ppm, respectively). In contrast, the shifts of −121.6, 58.4, and 121.8 ppm predicted by this equation for **2**$[PF_6]_2$, using

(60) Because of the different spin states of the di- and mononuclear paramagnetic Fe^{III} species (triplet vs doublet), halved A_H values are found for a similar atomic spin density in the dinuclear complexes.

(61) The regression coefficient of the fit becomes 0.97 and the slope 2.9 when the data for the monoradicals **4**$[PF_6]$ and **5**$[PF_6]$ are included in the plot.

(62) This certainly originates from the use of simplified compounds in the calculation,[63] from the tendency of DFT calculations to overemphasize spin delocalization,[64] and perhaps also from neglect of the local dipolar effect in our treatment of the experimental ^{1}H NMR data. [29] Moreover, the DFT calculations were presently conducted on a single conformation in a vacuum, without any counterion, whereas the experimental data were gathered on interconverting conformers in solution, which constitutes another potential source of discrepancy.

(63) Adamo, C.; Subra, R.; Di Matteo, A.; Barone, V. *J. Chem. Phys.* **1998**, *109*, 10244–10254.

(64) Ciofini, I.; Illas, F.; Adamo, C. *J. Chem. Phys.* **2004**, *120*, 3811–3816.

Chart 4. J_{ab} Values for Selected Organic Diradicals Related to **1**−**3**$[PF_6]_2$ and the VB Structure of the Thiele Diradical (**S-7**) in Its Singlet GS

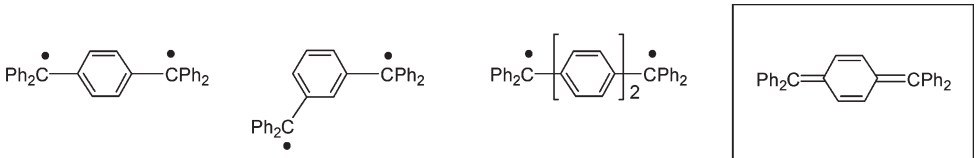

7 (J_{ab} << -250 cm^{-1}) **8** (J_{ab} > 450 cm^{-1}) **9** (J_{ab} ~ -275 cm^{-1}) **S-7**

the isotropic shifts of **4**$[PF_6]$, compare poorly with the shifts of −94.6, 42.6, and −94.3 ppm, respectively, experimentally observed. This clear discrepancy with eq 8 indicates that the spin distribution in each magnetic orbital that extends on the arylethynyl spacer in **2**$[PF_6]_2$ is not properly modeled by that of **4**$[PF_6]$. In contrast, for **1**$[PF_6]_2$ or **3**$[PF_6]_2$, the good agreement obtained confirms that the magnetic coupling does not induce a large perturbation of the electronic structure of the spin-carrying units in these dinuclear complexes relative to **4**$[PF_6]$ and **5**$[PF_6]$, respectively.

Exchange Coupling in 1−**3**$[PF_6]_2$. The 1,4-phenylene and 4,4′-biphenylene units are well-known antiferromagnetic couplers, while the 1,3-phenylene unit is a ferromagnetic one.[65] In accordance with these simple considerations,[66] antiferromagnetic interactions were experimentally evidenced for **1**$[PF_6]_2$ and **3**$[PF_6]_2$, while a ferromagnetic interaction was evidenced for **2**$[PF_6]_2$.

In the case of **1**$[PF_6]_2$, as was anticipated, the antiferromagnetic interaction is strong ($J_{ab} \approx -190$ cm^{-1}) and much larger than was previously found.[12,19] In the case of for **2**$[PF_6]_2$, the ferromagnetic coupling ($J_{ab} \geq +150$ cm^{-1}) is also significantly larger than was previously found.[11,16] The reasonably close J_{ab} values derived by DFT for the computationally simpler complexes **1**-H^{2+} (−255 cm^{-1}) and **2**-H^{2+} (+256 cm^{-1}) give further support to the existence of large exchange couplings in these dinuclear Fe^{III} compounds. The very weak antiferromagnetic coupling experimentally evidenced for **3**$[PF_6]_2$ ($J_{ab} \approx -1$ cm^{-1}) indicates that the large exchange interaction present in **1**$[PF_6]_2$ is severely depressed by the insertion of an additional 1,4-phenylene unit in the carbon-rich bridge. This is also qualitatively confirmed by DFT because a significantly smaller $|J_{ab}|$ value is computed for **3**-H^{2+} ($J_{ab} = -79$ cm^{-1}), although this computed value largely overestimates the experimental value obtained for **3**$[PF_6]_2$.[67]

The good match found for the singlet−triplet gaps ($2J_{ab}$) of **1**$[PF_6]_2$ in the solid state (SQUID) and in solution (VT-NMR) also reveals that the exchange coupling is only marginally affected by random molecular motions of this compound in solution, a remarkable feature in light of DFT computations recently conducted by Berke and co-workers on a related Mn^I diradicals, which evidenced a large sensitivity of the exchange coupling to conformational changes.[8] While establishing the essentially intramolecular origin of J_{ab}, these VT-NMR studies in solvents of different polarity also show that the exchange coupling is independent (within experimental error) of the dielectric medium surrounding **1**$[PF_6]_2$. This constitutes another noticeable feature of this dinuclear Fe^{III} complex,[4,28] which might explain the good correspondence stated between the experimental J_{ab} values determined for this compound and that computed for **1**-H^{2+}.

When compared to J_{ab} values classically derived for dinuclear polyradicals featuring two paramagnetic transition-metal ions, the values obtained for **1**$[PF_6]_2$ and **2**$[PF_6]_2$ are remarkable for their magnitude, even among carbon-rich diradicals,[27] and especially more for dinuclear compounds having metal centers more than 11 Å apart.[26] In line with previous findings,[4,6,7,13,68] this confirms that carbon-rich bridges are particularly suited to convey magnetic interactions between inorganic spin carriers over fairly large distances in organometallic diradicals involving group 8 transition metals.[11] Notably, although possessing large exchange couplings for organometallic diradicals, the dinuclear Fe^{III} complexes **1**-$[PF_6]_2$ and **2**$[PF_6]_2$ are apparently less coupled than their famous organic analogues, which are the Thiele (**7**) and Schlenk (**8**) hydrocarbons (Chart 4).[47,69]

Spin Delocalization and Magnetic Interactions for 1−**3**-$[PF_6]_2$. As was already shown in Scheme 1, the antiferromagnetic exchange coupling taking place for **1**$[PF_6]_2$ and **3**$[PF_6]_2$ can be rationalized considering that the "bonding" interaction between the unpaired spins is at the origin of stabilization of the singlet state. This interaction can take place only in the singlet state and is related to

(65) Rajca, A. *Chem. Rev.* **1994**, *94*, 871–893.

(66) (a) Ovchinnikov, A. O. *Theor. Chim. Acta* (*Berlin*) **1978**, *47*, 297–304. (b) Borden, W. T.; Iwamura, H.; Berson, J. A. *Acc. Chem. Res.* **1994**, *27*, 109–116.

(67) We tentatively relate this discrepancy to the overestimation of the spin density delocalized on the spacer in **3**-H^{2+} relative to that of the real compound, as suggested by the comparison of the theoretical versus experimental spin densities found on the second ring for **5**-H^+ and **5**$[PF_6]$ (compare Table 3 and Chart 5).

(68) (a) Pardo, E.; Carrasco, R.; Ruiz-Garcia, R.; Julve, M.; Lloret, F.; Munoz, M. C.; Journaux, Y.; Ruiz, E.; Cano, J. *J. Am. Chem. Soc.* **2008**, *130*, 576–585. (b) Cotton, F. A.; Murillo, C. A.; Young, M. D.; Yu, R.; Zhao, Q. *Inorg. Chem.* **2008**, *47*, 219–229. (c) Gao, L.-B.; Khan, J.; Fan, Y.; Zhang, L.-Y.; Liu, S.-H.; Chen, Z.-N. *Inorg. Chem.* **2007**, *46*, 5651–5664. (d) Min, K. S.; Reingold, A. L.; DiPasquale, A.; Miller, J. S. *Inorg. Chem.* **2006**, *45*, 6135–6137.

(69) The singlet−triplet gap $|2J_{ab}|$ could never be determined for **7** because of its high reactivity but is believed to be much larger than 500 cm^{-1},[70] while that for **9** was too large to be experimentally derived.[71] Recent computational estimates suggest that it lies around 900 cm^{-1}.[65] Although some controversy has arisen about the magnitude of this value,[47,72,73] the singlet−triplet gap of the Tschibtschibabin hydrocarbon **9** was experimentally estimated to be around 750 ± 100 cm^{-1}.[70]

(70) Brauer, H.-D.; Stieger, H.; Hartmann, H. *Z. Phys. Chem. Neue Folge* **1969**, *63*, 50–65.

(71) (a) Luckhurst, G. R.; Pedulli, G. F. *J. Chem. Soc. B* **1971**, 329–334. (b) Kothe, G.; Denkel, K.-H.; Summermann, W. *Angew. Chem., Int. Ed. Engl.* **1970**, *9*, 906–907.

(72) Montgomery, L. K.; Huffman, J. C.; Jurczak, E. A.; Grendze, M. P. *J. Am. Chem. Soc.* **1986**, *108*, 6004–6011.

(73) Popp, F.; Bickelhaupt, F.; Maclean, C. *Chem. Phys. Lett.* **1978**, *55*, 327–330.

Scheme 2. Singlet−Triplet Gaps generated by Antiferromagnetic Coupling between Unpaired Spins in **1**$[PF_6]_2$ and **3**$[PF_6]_2$ and by Ferromagnetic Coupling in **2**$[PF_6]_2$

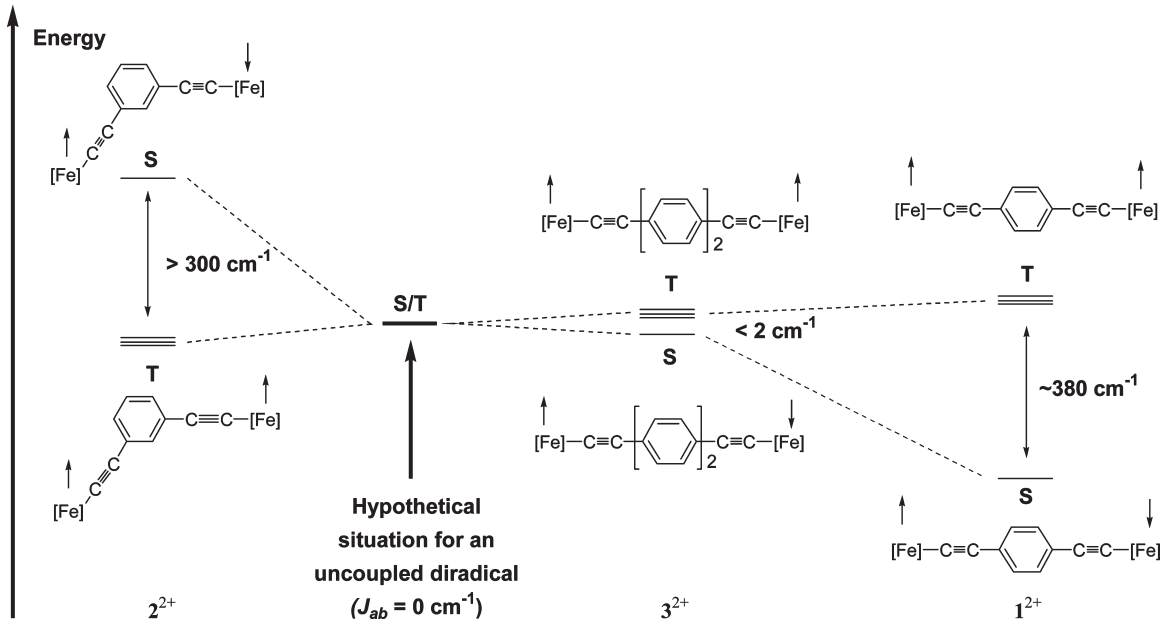

Scheme 3. (a) VB Representation of **1**$[PF_6]_2$ and **3**$[PF_6]_2$ Allowing One To Understand the Possible Origin of the Antiferromagnetic Coupling Operative in These Diradicals and (b) Equivalent VB Representation To Describe the Spin Delocalization in Functional Analogues of **4**$[PF_6]_2$ and **5**$[PF_6]_2$

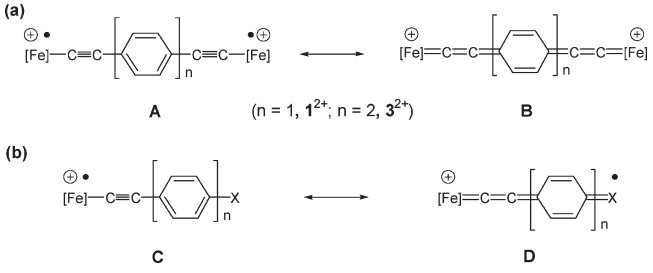

delocalization of the unpaired spins on the bridging 1,4-phenylene unit(s).[74] As is presently observed with **2**$[PF_6]_2$, such an interaction cannot happen with a 1,3-phenylene spacer because of the symmetry of the frontier molecular orbitals of this fragment.[75] In a VB formalism, this interaction results in an increasing weight of the cumulenic/quinoidal mesomer B in the description of the singlet state (Scheme 3). Such a description is well in line with the work previously done on mononuclear Fe^{III} compounds, for which the spin delocalization on the arylethynyl ligand has been related to the increasing weight of the cumulene-based structure D.[38,76] However, while the pairing interaction corresponds to the formation of the new bond in B and constitutes a stabilizing interaction, the energetic gain resulting from this interaction is balanced by the energetic cost of breaking the aromaticity of the phenyl ring(s), a cost improving with the number of 1,4-phenylene rings in the polyynediyl bridge. This type of competition between two limiting VB mesomers is a recurrent question for rationalizing the electronic properties of diradicals featuring polyphenylene bridges.[72,75,77] In this respect, it has been established that longer polyphenylene-based diradicals will usually present a dominant diradicalar structure, while shorter ones will present a dominant quinoidal structure, with the "turning" point being usually around two of three aryl rings depending on the nature of the terminal radical units.[78] Thus, terminal units X favoring spin delocalization will favor stronger quinoidal weights and maintain such a character over longer poly(1,4-phenylene) bridges.

Considering that the spin delocalization in the mononuclear complexes **4**$[PF_6]$ and **5**$[PF_6]$ reasonably models that taking place from each Fe^{III} center in the corresponding dinuclear complexes **1**$[PF_6]_2$ and **3**$[PF_6]_2$, respectively, it was interesting to have a closer look at the isotropic hyperfine coupling constants of the aromatic arylethynyl protons for these compounds.[29,53] These indicate that comparable spin densities are delocalized on the phenyl ring directly linked to the acetylide spacer in **4**$[PF_6]$ and **5**$[PF_6]$, while a more than 6-fold decrease in the spin density is experimentally evidenced on the second phenyl ring in **5**$[PF_6]$ relative to the first one (Table 2). Thus, the overlap between the delocalized spin densities of opposite signs per phenylene unit of the bridge should be more limited for **3**$[PF_6]_2$ than for **1**$[PF_6]_2$. The stabilizing pairing interaction, represented by mesomer B in Scheme 3, should therefore take place to a more limited extent for **3**$[PF_6]_2$, explaining in a qualitative way why the antiferromagnetic coupling for this diradical is strongly

(74) Kahn, O. *Molecular Magnetism*; VCH Publisher Inc.: New York, 1993.
(75) Hiberty, P. C.; Karafiloglou, P. *Theor. Chim. Acta* (*Berlin*) **1982**, *61*, 171–177.
(76) For related Ru^{III}-based examples, see: (a) Paul, F.; Ellis, B. J.; Bruce, M. I.; Toupet, L.; Roisnel, T.; Costuas, K.; Halet, J.-F.; Lapinte, C. *Organometallics* **2006**, *25*, 649–665. (b) Gauthier, N.; Tchouar, N.; Justaud, F.; Argouarch, G.; Cifuentes, M. P.; Toupet, L.; Touchard, D.; Halet, J.-F.; Rigaut, S.; Humphrey, M. G.; Costuas, K.; Paul, F. *Organometallics* **2009**, *28*, 2253–2266.
(77) (a) Karafiloglou, P. *Int. J. Quantum Chem.* **1984**, *25*, 293–308. (b) Jacobs, S. J.; Schultz, D. A.; Jain, R.; Novak, J.; Dougherty, D. A. *J. Am. Chem. Soc.* **1993**, *115*, 1744–1753. (c) Silverman, S. K.; Dougherty, D. A. *J. Phys. Chem.* **1993**, *97*, 13273–13283.
(78) Guihery, N.; Maynau, D.; Malrieu, J.-P. *Chem. Phys. Lett.* **1996**, *248*, 199–206.

Chart 5. Isotropic Hyperfine Coupling Constants of Hydrogen Atoms (A_H) for the Organometallic Radicals $\mathbf{4}^+$ and $\mathbf{5}^+$ Compared to Those of Related Organic Radicals, Such as **10** and **11** (in G)

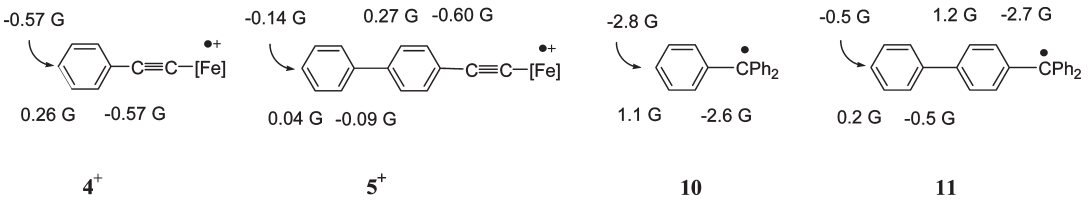

$\mathbf{4}^+$ $\mathbf{5}^+$ **10** **11**

decreased relative to that operative in $\mathbf{1}[PF_6]_2$. Along the same lines, the comparison of these data with the hyperfine couplings determined for the organic radicals **10** and **11** can be traced back to the comparably stronger exchange couplings taking place in the corresponding organic diradicals **7** and **9** (Chart 5).[29,38]

On a different footing, according to Anderson,[79] the magnitude of the antiferromagnetic exchange in dinuclear diradicals is often supposed to be induced by the intramolecular electron transfer between the metallic end groups and can then be related to the electronic coupling or transfer integral (H_{ab}) between the magnetic orbitals. This transfer integral for the diradical is usually supposed to be similar to that determined for the one-electron-reduced mixed-valence complex. In that respect, several relations between J_{ab} for a given antiferromagnetically coupled diradical and the electronic coupling in the corresponding mixed-valence complex have been put forward,[4,6,80] such as eq 9, initially proposed by Bertrand.[81] According to this expression, the antiferromagnetic exchange coupling should scale as the squared electronic coupling (H_{ab}) in the corresponding mixed-valence complexes and inversely to the energy of the intervalence charge-transfer (MMCT) band in the dication.[6] The former quantities were recently determined for $\mathbf{1}[PF_6]$ and $\mathbf{3}[PF_6]$ in solution (H_{ab} = 1700 and 145 cm^{-1}),[17] but the energy of the MMCT transition in the diradicals is currently not known. Nevertheless, on the basis of the available H_{ab} data, a ca. 150-fold decrease of the antiferromagnetic exchange coupling (J_{ab}) between $\mathbf{1}[PF_6]_2$ and $\mathbf{3}[PF_6]_2$ can be expected from eq 8 for a constant MMCT band energy. An even larger decrease might take place if the MMCT state for $\mathbf{3}[PF_6]_2$ is slightly higher in energy than that for $\mathbf{1}[PF_6]_2$, which constitutes a possible situation. Thus, the decrease of J_{ab} when progressing from $\mathbf{1}[PF_6]_2$ to $\mathbf{3}[PF_6]_2$ is perhaps also related to the decrease in the electronic delocalization between the Fe^{III} centers, especially when considering the large experimental uncertainties surrounding the J_{ab} value determined for $\mathbf{3}[PF_6]_2$.

$$J_{ab} = (H_{ab})^2/\overline{\nu}_{CT} \quad (9)$$

Spin Delocalization and Structural Changes between Spin Isomers for $\mathbf{1}-\mathbf{3}[PF_6]_2$. The possible geometrical changes taking place on the carbon-rich bridge between the triplet and singlet states were also of major interest to us. On the basis of Scheme 3, the stabilization of the singlet state of $\mathbf{1}[PF_6]_2$ or $\mathbf{3}[PF_6]_2$ results from the resonance with the closed-shell singlet mesomer B. When large, this interaction might therefore impart some cumulenic/quinoidal character to the bridging spacer specifically in their singlet states. In order to experimentally check the occurrence of such a phenomenon, we have closely investigated the temperature-dependent changes in the spectroscopic signatures of the strongly coupled diradicals $\mathbf{1}[PF_6]_2$ and $\mathbf{2}[PF_6]_2$.[82] No clear evidence for any structural change could be gained from UV−Vis−near-IR investigations between 298 and 10 K. However, in line with the diffraction data gathered on this complex,[85] a very weak and reversible rearrangement toward a more cumulenic/quinoidal structure is suggested by VT-IR selectively for $\mathbf{1}[PF_6]_2$ upon a decrease in the temperature.[87] Indirect support for a larger cumulenic/quinoidal character of $\mathbf{1}[PF_6]_2$ in the singlet state is also provided by the DFT calculations, which reveal consistent differences between the optimized geometries computed for the T and BS states of $\mathbf{1}\text{-}H^{2+}$ (Supporting Information).[56] Again, these computed structural changes remain very slight, even for the strongly coupled diradical $\mathbf{1}\text{-}H^{2+}$. Thus, the expected structural changes of the carbon-rich spacer in the singlet state based on VB considerations (Scheme 3) appear to actually take place for $\mathbf{1}[PF_6]_2$ but

(79) Anderson, P. W. *Phys. Rev.* **1959**, *115*, 2–13.

(80) (a) Nelsen, S. F.; Ismaglilov, R. F.; Teki, Y. *J. Am. Chem. Soc.* **1998**, *120*, 2200–2201. (b) Evans, C. E. B.; Naklicki, M. L.; Rezvani, A. L.; White, C. A.; Kondratiev, V. V.; Crutchley, R. J. *J. Am. Chem. Soc.* **1998**, *120*, 13096−13103 and references cited therein.

(81) Bertrand, P. *Chem. Phys. Lett.* **1985**, *113*, 104–107.

(82) Vibrational[83] and electronic[84] spectroscopies are well-known to constitute accurate reporters of bonding changes between spin isomers.

(83) (a) Casado, J.; Patchkovskii, S.; Zgierski, M. Z.; Hermosilla, L.; Sieiro, C.; Oliva, M. M.; Navarrete, J. T. L. *Angew. Chem., Int. Ed.* **2008**, *47*, 1443–1446. (b) Ortiz, R. P.; Casado, J.; Hernandez, V.; Navarete, J. T. L.; Viruela, P. M.; Orti, E.; Takimiya, K.; Otsubo, T. *Angew. Chem., Int. Ed.* **2007**, *46*, 9057–9061.

(84) (a) Mathonière, C.; Kahn, O.; Daran, J.-C.; Hilbig, H.; Köhler, F. H. *Inorg. Chem.* **1993**, *32*, 4057–4062. (b) Mathonière, C.; Kahn, O. *Inorg. Chem.* **1994**, *33*, 2103–2108.

(85) Based on bond lengths measured for $\mathbf{1}[PF_6]_2$ and published bond-length values,[72,86] the maximal cumulenic/quinoidal contribution is estimated at around 20% for this diradical.[78] A lower quinoidal character is apparent from the bond lengths measured for $\mathbf{3}[PF_6]_2$ at 120 K,[17] but no sensible value could be determined in this case.

(86) Orpen, A. G.; Brammer, L.; Allen, F. H.; Kennard, O.; Watson, D. G.; Taylor, R. *J. Chem. Soc., Dalton Trans.* **1989**, S1–S83.

(87) The Mössbauer data also suggest that minimal changes take place because quite close quadrupolar splittings were reported for these three diradicals (QS = 0.91,[15,17] 0.89,[16,88] and 0.89 mm s^{-1} for $\mathbf{1}-\mathbf{3}[PF_6]_2$, respectively) and for the mononuclear complex $\mathbf{4}[PF_6]$ (0.90 mm s^{-1}) at 80 K.[89] More significant differences would have been expected at that temperature for $\mathbf{1}[PF_6]_2$ in the case of a pronounced cumulenic/quinoidal structural change of the carbon-rich bridge.[11,90]

(88) Weyland, T.; Costuas, K.; Toupet, L.; Halet, J.-F.; Lapinte, C. *Organometallics* **2000**, *19*, 4228–4239.

(89) Connelly, N. G.; Gamasa, M. P.; Gimeno, J.; Lapinte, C.; Lastra, E.; Maher, J. P.; Le Narvor, N.; Rieger, A. L.; Rieger, P. H. *J. Chem. Soc., Dalton Trans.* **1993**, 2575–2578.

(90) (a) Guillaume, V.; Thominot, P.; Coat, F.; Mari, A.; Lapinte, C. *J. Organomet. Chem.* **1998**, *565*, 75–80. (b) Guillaume, V.; Mahias, V.; Mari, A.; Lapinte, C. *Organometallics* **2000**, *19*, 1422–1426.

remain close to the limit of experimental detection, even when $|J_{ab}|$ is as high as 190 cm^{-1}.

Such a statement is at odds with the situation prevailing for related d^5-based organometallic diradicals containing polyynediyl spacers (Scheme 1a)[11,13,14] or featuring a 9,10-anthryl group in place of the 1,4-phenylene unit(s) (**6**$[PF_6]_2$ in Chart 1).[9] According to the preceding section, this can be related to the larger spin delocalization taking place on the carbon-rich spacer and to the larger antiferromagnetic exchange coupling in this diamagnetic complex ($J_{ab} \ll -500$ cm^{-1}).[20] Also, the Thiele (**7**) and Tschtichibabin (**9**) organic diradicals present a comparably more marked quinoidal character than **1**$[PF_6]_2$ and **3**$[PF_6]_2$, in line with the larger antiferromagnetic interactions evidenced for these compounds.[72] Actually, when compared to purely organic diradicals, **1**$[PF_6]_2$ and **3**$[PF_6]_2$ are more reminiscent of bis(triarylaminium) or anthryl-bridged verdazyl diradicals,[91] for which very small structural changes between singlet and triplet spin isomers have been evidenced, in spite of comparable intramolecular exchange couplings.

Conclusions

In this contribution, we have used magnetic susceptibility measurements (SQUID), NMR, and DFT to study the magnetic properties and electronic structures of the organometallic diradicals **1**−**3**$[PF_6]_2$.

Upon comparison to other inorganic or organometallic diradicals, remarkably strong intramolecular exchange interactions were evidenced between the two unpaired electrons of the two former compounds. Thus, an antiferromagnetic coupling of ca. −190 cm^{-1} was found for **1**$[PF_6]_2$, while a ferromagnetic coupling of ca. 150 cm^{-1} or larger was evidenced for **2**$[PF_6]_2$. A much weaker antiferromagnetic interaction ($0 > J_{ab} \gg -1$ cm^{-1}) takes place in the solid state for **3**$[PF_6]_2$, which possesses an additional 1,4-phenylene unit inserted in the bridge. In line with the previous results, this study confirms the outstanding capability of carbon-rich bridges containing a single phenylene unit to efficiently convey magnetic interactions over large distances (≥11 Å) as well as is the determining influence of the phenylene substitution pattern (i.e., 1,4 vs 1,3 substitution) on the nature of the magnetic interaction (i.e., antiferro- vs ferromagnetic coupling, respectively).

We also conclusively show here that the GS structure of **1**$[PF_6]_2$ retains a pronounced diradical character in spite of the relatively strong antiferromagnetic exchange coupling evidenced. Likewise, a dominant diradical character is demonstrated for **3**$[PF_6]_2$ in the GS. This investigation thereby definitively establishes that the structural changes between the singlet and triplet states for organoiron diradicals featuring 1,4-phenylene units in the bridge will remain very slight, in marked contrast to the results previously reported for the analogue of **1**$[PF_6]_2$ featuring a 9,10-anthryl unit (**6**$[PF_6]_2$) or for the related organic Thiele diradical **7**. On the basis of DFT calculations and NMR measurements, we point out that these differences likely originate from the lesser delocalization of the unpaired electrons on the bridging ligands in **1**$[PF_6]_2$ and **3**$[PF_6]_2$ relative to **6**$[PF_6]_2$ or **7**.

Finally, and in a more general way, we also hope to have shown that NMR can prove very complementary to SQUID measurements for investigating magnetic interactions across various organic bridges, especially when organometallic end groups featuring metallic centers with fast-relaxing d electrons, such as "$[(\eta^2\text{-dppe})(\eta^5\text{-}C_5Me_5)Fe]^+$" fragments, act as spin carriers. Moreover, in contrast to SQUID measurements, NMR is well suited to study samples contaminated with traces of paramagnetic species. In such instances, this technique constitutes a rapid and convenient way to extract important information regarding the spin distribution on the bridging spacer. The magnitude of the intramolecular exchange interaction can also be obtained in favorable cases. We now intend to use this technique in a more systematic way for similar investigations on related compounds in the future.

Experimental Section

General Data. All manipulations were carried out under inert atmospheres. Solvents or reagents were used as follows: Et_2O and *n*-pentane, distilled from Na/benzophenone; CH_2Cl_2, distilled from CaH_2 and purged with argon; $HN(^iPr)_2$, distilled from KOH and purged with argon; aryl bromides (Acros, >99%), opened/stored under argon. The direct-current magnetic susceptibility measurements were performed on a solid polycrystalline sample with a Quantum Design MPMS-XL SQUID magnetometer between 2 and 300 K. These measurements were all corrected for the diamagnetic contribution as calculated with Pascal's constants. Transmittance FTIR spectra were recorded using a Bruker IFS28 spectrometer (400−4000 cm^{-1}). The low-temperature absorption measurements were performed using a Varian Cary 5E double-beam spectrophotometer equipped with an APD Cryogenics closed-cycle helium cryogenic system including a DMX-1E cryostat and a DE-202 expander. All NMR experiments were made on a Bruker AVANCE 500 operating at 500.15 MHz for ^1H and 125.769 MHz for ^{13}C, with a 5 mm broad band observation probe equipped with a *z*-gradient coil (see the Supporting Information).[29] The complexes **1**−**5**$[PF_6]$[17] were obtained as previously reported.

Crystallography. Crystals of **1**$[PF_6]_2\cdot CH_2Cl_2$ were studied on an Oxford Diffraction Xcalibur Saphir 3 with graphite-monochromatized Mo Kα radiation at 100 and 293 K. The cell parameters were obtained with Denzo and Scalepack with 10 frames (ψ rotation: 1° per frame).[92] The data collection[93] ($2\theta_{max}$, number of frames, Ω rotation, scan rate, and *hkl* range are given in Table 4) provided reflections for **1**$[PF_6]_2\cdot CH_2Cl_2$. Subsequent data reduction with Denzo and Scalepack[92] gave independent reflections (Table 4). The structures were solved with *SIR-97*, which revealed the non-hydrogen atoms.[94] After anisotropic refinement, the remaining atoms were found in Fourier difference maps. The complete structures were then refined with *SHELXL97*[95] by the full-matrix least-squares technique (use of the F^2 magnitude; *x*, *y*, *z*, β_{ij} for iron, phophorus, carbon, nitrogen, and/or oxygen atoms, *x*, *y*, *z* in riding mode for hydrogen atoms, with variables "*N*(var.)", observations, and "*w*" used as defined in Table 4). Atomic scattering factors were

(91) (a) Zheng, S.; Barlow, S.; Risko, C.; Kinnibrugh, T. L.; Khrustalev, V. N.; Jones, S. C.; Antipin, M. Y.; Tucker, N. M.; Timofeeva, T. V.; Coropceanu, V.; Bredas, J.-L.; Marder, S. R. *J. Am. Chem. Soc.* **2006**, *128*, 1812–1817. (b) Ciofini, I.; Lainé, P. P.; Zamboni, M.; Daul, C. A.; Marvaud, V.; Adamo, C. *Chem.—Eur. J.* **2007**, *13*, 5360–5377.

(92) Otwinowski, Z.; Minor, W. In *Methods in Enzymology*; Carter, C. W., Sweet, R. M., Eds.; Academic Press: London, 1997; Vol. *276*, pp 307−326.

(93) *Kappa CCD Software*; Nonius BV: Delft, The Netherlands, 1999.

(94) Altomare, A.; Burla, M. C.; Camalli, M.; Cascarano, G.; Giacovazzo, C.; Guagliardi, A.; Moliterni, A. G. G.; Polidori, G.; Spagna, R. *J. Appl. Chem.* **1998**, *31*, 74–77.

(95) Sheldrick, G. M. *SHELX97-2: Program for the refinement of crystal structures*; Universitat Göttingen: Göttingen, Germany, 1997.

taken from the literature.[96] ORTEP views of $\mathbf{1}^{2+}$ were realized with *PLATON98*.[97]

Magnetic Susceptibility Measurements (SQUID). Crushed crystalline samples of $\mathbf{1}[PF_6]_2$ and $\mathbf{3}[PF_6]_2$ previously sonicated and washed in diethyl ether were subjected to SQUID measurements. For $\mathbf{2}[PF_6]_2$, a freshly prepared (powderish) sample was used. The data were fitted using a modified Bleaney−Bowers law as described above (eq 2).

VT-IR and UV−Vis−Near-IR Measurements. Small amounts of microcrystalline solids were handled under argon (glovebox), mixed with ground KBr, and used for the preparation of KBr pellets.

NMR Experiments. The ^{1}H NMR spectra were recorded between 100 and −150 ppm using ca. $(1-5) \times 10^{-2}$ M solutions of the compounds in dichloromethane-d^2. The ^{13}C NMR spectra were recorded between 1000 and −300 ppm using similar solutions.

Computational Details. DFT calculations were performed with the *Gaussian03* program.[98] All geometries were optimized without any symmetry constraint. The functional used is B3LYP.[99] The atomic basis set employed is the LANL2DZ ECP basis set, augmented with a polarization function for all atoms except hydrogen atoms.[100] The guess functions of the BS systems were generated with the *Jaguar 6.0* code.[101]

Acknowledgment. Antoine Tissot is acknowledged for experimental assistance and Dr. Claude Lapinte (UMR CNRS 6226) is acknowledged for discussions. The CINES and IDRIS-CNRS are acknowledged for computing facilities. The CNRS is acknowledged for financial support.

Supporting Information Available: Additional spectroscopic (NMR and UV−Vis−near-IR) data on $\mathbf{1}-\mathbf{3}[PF_6]_2$, Cartesian coordinates of all DFT-optimized geometries for $\mathbf{1}$-H^{2+}, $\mathbf{2}$-H^{2+}, $\mathbf{3}$-H^{2+}, $\mathbf{4}$-H^{+}, and $\mathbf{5}$-H^{+}, comparison between selected theoretical and experimental bonding parameters and angles for $\mathbf{1}$-H^{2+} and $\mathbf{3}$-H^{2+}, derivation of spin densities for selected aromatic protons based on isotropic shifts, derivation of eqs 4c and 8, and CIF of $\mathbf{1}[PF_6]_2 \cdot CH_2Cl_2$. This material is available free of charge via the Internet at http://pubs.acs.org. Final atomic positional coordinates, with estimated standard deviations, bond lengths and angles, and anisotropic thermal parameters, have been deposited at the Cambridge Crystallographic Data Centre and allocated the deposition number CCDC 298750. The coordinates can be obtained, upon request, from the Director, Cambridge Crystallographic Data Centre, 12 Union Road, Cambridge CB2 1EZ, U.K.

(96) Reidel, D. *International Tables for X-ray Crystallography*; Kynoch Press (presently distributed by D. Reidel, Dordrecht, The Netherlands): Birmingham, AL, 1974; Vol. *IV*.

(97) Spek, A. L. *PLATON: A Multipurpose Crystallographic Tool*; Utrecht University: Utrecht, The Netherlands, 1998.

(98) Frisch, M. J. T. G. W.; Schlegel, H. B.; Scuseria, G. E.; Robb, M. A.; Cheeseman, J. R.; Montgomery, J. A., Jr.; Vreven, T.; Kudin, K. N.; Burant, J. C.; Millam, J. M.; Iyengar, S. S.; Tomasi, J.; Barone, V.; Mennucci, B.; Cossi, M.; Scalmani, G.; Rega, N.; Petersson, G. A.; Nakatsuji, H.; Hada, M.; Ehara, M.; Toyota, K.; Fukuda, R.; Hasegawa, J.; Ishida, M.; Nakajima, T.; Honda, Y.; Kitao, O.; Nakai, H.; Klene, M.; Li, X.; Knox, J. E.; Hratchian, H. P.; Cross, J. B.; Bakken, V.; Adamo, C.; Jaramillo, J.; Gomperts, R.; Stratmann, R. E.; Yazyev, O.; Austin, A. J.; Cammi, R.; Pomelli, C.; Ochterski, J. W.; Ayala, P. Y.; Morokuma, K.; Voth, G. A.; Salvador, P.; Dannenberg, J. J.; Zakrzewski, V. G.; Dapprich, S.; Daniels, A. D.; Strain, M. C.; Farkas, O.; Malick, D. K.; Rabuck, A. D.; Raghavachari, K.; Foresman, J. B.; Ortiz, J. V.; Cui, Q.; Baboul, A. G.; Clifford, S.; Cioslowski, J.; Stefanov, B. B.; Liu, G.; Liashenko, A.; Piskorz, P.; Komaromi, I.; Martin, R. L.; Fox, D. J.; Keith, T.; Al-Laham, M. A.; Peng, C. Y.; Nanayakkara, A.; Challacombe, M.; Gill, P. M. W.; Johnson, B.; Chen, W.; Wong, M. W.; Gonzalez, C.; Pople, J. A. *Gaussian 03*, revision C02; Gaussian, Inc.: Wallingford, CT, 2004.

(99) (a) Mielich, B.; Savin, A.; Stoll, H.; Preuss, H. *Chem. Phys. Lett.* **1989**, *157*, 200. (b) Lee, C.; Yang, W.; Parr, R. G. *Phys. Rev. B* **1988**, *37*, 785. (c) Becke, A. D. *J. Chem. Phys.* **1993**, *98*, 5648.

(100) Hay, P. J.; Wadt, W. R. *J. Chem. Phys.* **1985**, *82*, 270–299.

(101) *Schrodinger*, 6.0 ed.; LLC: New York, 2005.